UNIVERSITÀ DEGLI STUDI DI PADOVA

Università degli Studi di Padova

Dipartimento di Scienze del Farmaco

SCUOLA DI DOTTORATO DI RICERCA IN SCIENZE FARMACOLOGICHE

INDIRIZZO FARMACOLOGIA, TOSSICOLOGIA E TERAPIA

XXVIII ciclo

ACTIVATION PHENOTYPES OF HUMAN MONOCYTE-DERIVED MACROPHAGES: METHODOLOGICAL APPROACHES AND PHARMACOLOGICAL MODULATION BY CURCUMIN ANALOGUES

Direttore della Scuola: Ch.mo Prof. Pietro Giusti

Coordinatore d'indirizzo: Ch.mo Prof. Pietro Palatini

Supervisore: Ch.mo Prof. Andrea Cignarella

Dottoranda: Serena Tedesco

" Pensò a tutta la strada che aveva fatto,
e alla strana maniera in cui Dio
gli aveva mostrato il tesoro.
Se non avesse creduto ai sogni che si ripetevano,
non avrebbe incontrato la zingara,
il re, il rapinatore o... "Be', la lista è molto lunga.
Ma il cammino era indicato dai segnali,
e io non potevo sbagliare", disse fra se e se. "
-L'alchimista, Paolo Coehlo-

INDEX

Abstract

Under normal conditions macrophages provide immune surveillance and host defense in tissues to maintain homeostasis. However, upon sensing changes in the microenvironment, macrophages become activated, undergoing a morphological and functional switch. Activation of these cells is not an “all-or-none” process, but rather a *continuum* characterized by a wide spectrum of molecular and functional phenotypes ranging from the “classical” M1 activated phenotype, with a highly pro-inflammatory profile, to the “alternative” M2 phenotype, associated with a beneficial, less inflammatory, protective profile. The possibility to promote a macrophage protective phenotype has therefore become a therapeutic goal in the treatment of inflammatory conditions, and the identification of factors that control cell activation is currently an area of active research. Most studies in the field so far have been performed using primary mouse macrophages or macrophage cell lines, and a variety of monocyte differentiation protocols and macrophage activation markers are used by different labs. Moreover, the pharmacological control of human macrophage polarized activation has not been extensively explored. A number of natural and synthetic compounds, including chalcones and curcumin, the major active component isolated from the turmeric plant *Curcuma longa*, have been shown to induce effects on macrophage function (including antioxidant, anti-microbial, anti-carcinogenic and anti-inflammatory action) through multiple pharmacological mechanisms, including interference with TLR4 signaling. On these grounds, the specific aims of the present thesis were: a) to test cell models and differentiation protocols other than spontaneous blood-derived macrophage differentiation, namely the THP-1 cell line and CSF-1-driven differentiation, respectively; b) to profile the cytokine pattern into the culture medium, and c) to determine the modulation of phenotypic markers by pharmacological agents, namely curcumin derivatives known to suppress microglial activation through reduced production and release of pro-inflammatory mediators, as well as the underlying mechanisms of action.

Macrophages were differentiated from human PBMCs isolated by density gradient centrifugation, and cultured in RPMI 1640 medium with 10% FBS with CSF-1 for 6 days to obtain resting macrophages (M0). Classical (M1) and alternative (M2) phenotypes were generated using specific cytokines (0.1-1 µg/ml LPS or 20 ng/ml IL-4 plus 5 ng/ml IL-13, respectively) in the presence or absence of curcumin analogues or dexamethasone used a reference compound. Macrophage phenotypes were determined by flow cytometry using fluorocrome-labeled antibodies. Gene expression was analysed using qRT-PCR. The composition of macrophage conditioned media (MCM) was assessed with the Luminex technology. Curcumin analogues were kindly provided by Dr. Federica Belluti (University of Bologna).

When M2 polarization was induced with IL-4/IL-13 for 24h, we observed increased expression of M2 markers compared with M0. In terms of gene expression analysis of the CSF-1 driven macrophages, as expected, M1-polarized macrophages after 6 or 48 h showed higher mRNA levels of TNF-α and IL-1β compared with M0. The increase in mRNA was more marked after 48 h for all genes except TNF-α, which rose more sharply after 6 h. The anti-inflammatory cytokine IL-10 mRNA was unexpectedly more abundant in M1- than in M2-polarized macrophages, and peaked after 6 h. Compared with M0, M2 MCM showed higher levels of anti-inflammatory cytokines including CCL22 and IL-4. In contrast, M1 MCM was associated with higher levels of IL-1α, IL-1β, IL-6, IL-8, MCP-1, VEGF and TNF-α. Treatment with the curcumin analogue GG9 as well as CLI095, an inhibitor of TLR4 intracellular domain, reversed the LPS-induced up-regulation of $CD80^+$ (M1) cells. A similar effect was maintained with the double positive $CD80^+/CCR2^+$ population. Unlike dexamethasone, which increased the percentage of $CD163^+$ (M2) cells, the curcumin analogue GG9 did not affect M2 markers. Treatment with GG9 significantly blocked IL-1β cytokine production at the cell-bound level, in the protein lysate and in the medium. By contrast, curcumin and GG6 did not affect the levels of intra- and extracellular IL-1β. To investigate intracellular signaling pathways involved in cell activation, we performed Western blot analysis of factors involved in the NF-κB pathway. Activation with LPS significantly decreased the relative expression of IκB-α. By contrast, curcumin and GG6 were able to restore IκB-α amounts as did CLI095, whereas no effect was induced by GG9 treatment.

Therefore, M1 and M2 macrophages showed specific profiles of gene expression and surface markers, which were modulated by pharmacological treatment with dexamethasone or a curcumin analogue. Overall, these data suggest that polarized activation protocols may have an impact on the functional status of macrophages and are critical to further investigate pharmacological macrophage targeting.

Riassunto

In condizioni normali i macrofagi sono i responsabili della risposta immunitaria e della difesa dell'ospite per mantenere l'omeostasi tissutale. In seguito a stimoli presenti nel microambiente, i macrofagi possono attivarsi, andando incontro a uno *switch* morfologico e funzionale. L'attivazione di queste cellule non è un processo "tutto o nulla" ma piuttosto un *continuum* caratterizzato da un ampio spettro di fenotipi molecolari e funzionali, i cui estremi sono rappresentati dal fenotipo definito "classico" o M1, con un profilo pro-infiammatorio, e da quello "alternativo" o M2, anti-infiammatorio e protettivo. La possibilità di promuovere un fenotipo macrofagico protettivo sta diventando un obiettivo terapeutico nel trattamento delle condizioni infiammatorie e l'identificazione di fattori che regolano l'attivazione cellulare è attualmente un'area di ricerca molto attiva. La maggior parte degli studi in questo ambito sono stati condotti utilizzando culture primarie di macrofagi di topo o linee cellulari; inoltre, i vari laboratori usano protocolli diversi di isolamento/differenziamento dei monociti e marcatori diversi di attivazione. Inoltre, il controllo farmacologico dell'attivazione macrofagica non è ancora stato indagato sufficientemente. Una serie di composti naturali e sintetici, ad esempio il calcone e la curcumina, il principale componente attivo della *Curcuma longa* (pianta nota per effetti anti-ossidanti, anti-microbici, anti-tumorali e anti-infiammatori) hanno dimostrato un effetto sulla funzione dei macrofagi, agendo attraverso diversi meccanismi farmacologici, ad esempio interferendo con il *signaling* del TLR4. Sulla base di queste premesse, gli scopi specifici di questo lavoro di tesi erano: a) testare un modello cellulare e un protocollo di differenziamento diverso da quello spontaneo, in particolare la linea cellulare monocitaria THP-1 e il differenziamento in presenza di CSF-1; b) determinare il profilo delle citochine presenti nel terreno di coltura e c) determinare la modulazione dei marcatori dei fenotipi di attivazione da parte di agenti farmacologici, in particolare da derivati di sintesi della curcumina, noti per la loro capacità di modulare l'attivazione di cellule murine di microglia attraverso la riduzione della produzione e rilascio di mediatori pro-infiammatori.

I macrofagi sono stati differenziati a partire dai linfo-monociti umani isolati tramite gradiente di densità e coltivati in terreno RPMI + 10% FBS con aggiunta di CSF-1 per 6 giorni, ottenendo così macrofagi in condizioni basali (M0). Il fenotipo classico (M1) e il fenotipo alternativo (M2) sono stati ottenuti incubando i macrofagi M0 rispettivamente con 0.1-1 µg/ml LPS e IL-4 20 ng/ml + IL-13 5 ng/ml, in presenza o assenza di analoghi della curcumina, desametazone o CLI095, un inibitore del dominio intracellulare del TLR4 (questi ultimi utilizzati come composti di riferimento). I fenotipi macrofagici sono stati determinati tramite citofluorimetria utilizzando specifici anticorpi legati a fluorofori. L'espressione genica è stata valutata tramite qRT-PCR. La composizione dei terreni condizionati (*macrophage conditioned media,* MCM) è stata valutata con la tecnologia Luminex. Gli analoghi

della curcumina sono stati gentilmente forniti dalla Prof.ssa Federica Belluti (Università di Bologna). In seguito a polarizzazione per 24 h con IL-4/IL-13 abbiamo osservato un aumento dell'espressione dei marcatori M2 rispetto a M0. Per quanto riguarda l'espressione genica di macrofagi differenziati con CSF-1, come atteso, i macrofagi M1 dopo 6 o 48h presentavano livelli superiori di mRNA per TNF-α e IL-1β rispetto a M0. L'aumento dell'mRNA era più marcato dopo 48 h per tutti i geni tranne TNF-α, che raggiungeva il picco a 6h. L'mRNA della citochina anti-infiammatoria IL-10 inaspettatamente era più espresso nei macrofagi M1 rispetto a M2 e raggiungeva il picco dopo 6 h. Rispetto a M0, l'MCM M2 era caratterizzato da alti livelli di citochine anti-infiammatorie tra le quali CCL22 e IL-4. Al contrario, l'MCM M1 presentava livelli elevati di IL-1α, IL-1β, IL-6, IL-8, MCP-1, VEGF e TNF-α. Il pre-trattamento con l'analogo della curcumina GG9 e il controllo positivo CLI095 ha prevenuto l'aumento indotto da LPS del marcatore M1 CD80. Un effetto simile è mantenuto anche sulla frazione di cellule a doppia marcatura $CD80^{+}/CCR2^{+}$. Al contrario del desametazone, che aumenta la percentuale di cellule $CD163^{+}$ (M2), il GG9 non ha modulato i marcatori M2. Il trattamento con GG9 ha bloccato in maniera significativa la produzione di IL-1β valutata come citochina *cell-bound*, nel lisato cellulare o rilasciata nel terreno di coltura. Al contrario, l'analogo GG6 non ha modificato i livelli di IL-1β intra- ed extra-cellulare. Per indagare più nel dettaglio le vie di segnale coinvolte nell'attivazione di queste cellule, abbiamo effettuato analisi Western Blot di fattori coinvolti nella via di segnale di NF-κB. L'attivazione con LPS ha ridotto significativamente l'espressione relativa di IκB-α. Curcumina, GG6 e CLI095 hanno riportato IκB-α ai livelli di controllo, a differenza del GG9 che non modificava significativamente l'espressione di questa proteina.

Pertanto, i macrofagi M1 ed M2 presentano specifici profili di attivazione genica e di marcatori di superficie che possono essere modulati in seguito a trattamento farmacologico con desametazone o analoghi della curcumina. Nel complesso, questi dati suggeriscono che protocolli di attivazione macrofagica possono avere un impatto sullo stato funzionale di queste cellule e sono fondamentali per definire nuove strategie di *targeting* farmacologico nei macrofagi umani.

1. Introduction

1.1 IMMUNE SYSTEM: THE ESSENTIALS

The immune system is a network of cells, tissues and organs that work together to defend the body against attacks by "foreign" invaders: these are primarily microbes, i.e. tiny organisms such as bacteria, parasites and fungi that can cause infections. The inflammatory response usually has two components: an innate non adaptive response and an adaptive (acquired or specific) immunologic response (Delves and Roitt, 2000). Innate immunity, also called natural immunity, consists of several body's own mechanisms which are rapidly able to counteract pathogens invasion. The main components of the innate immunity are:

1. physical/chemical barriers such as cough reflex, enzymes in tears and skin oils, mucus, skin and stomach acid that keep out harmful materials from entering the body, thus forming the first line of defense in the immune response;
2. phagocytic cells, such as neutrophils and macrophages, and cells with cytotoxic activity, such as natural killer (NK). The phagocytic cells use a combination of degrading enzymes, antimicrobial peptides and reactive oxygen species to kill the invading microorganisms. In addition, they release signaling molecules that trigger an inflammatory response and begin to marshal the forces of the adaptive immune system;
3. circulating proteins, such as those included in the complement system or other mediators of the immune response;
4. several proteins, such as cytokines and chemokines, which regulate and coordinate many functions performed by cells of innate immunity.

In addition to innate immunity, exposure to infectious agents initiate more complex mechanisms belonging to the so-called acquired immunity, whose power and defensive ability increases with each subsequent exposure to the same pathogen. The cumulative effects triggered by the immune system to defend the body against the etiologic agent are known as inflammation. In the long term, however, the lack of resolution and the chronicity of inflammatory responses may contribute to the

development of a number of diseases including, among others, atherosclerosis (Moore et al., 2013) and obesity (Han et al., 2013).

1.2. THE MONOCYTE-MACROPHAGE SYSTEM

Monocytes, macrophages and dendritic cells (DCs) are part of the "mononuclear phagocyte system" (MPS), a body-wide specialized system of phagocytic cells (van Furth et al., 1972). This system function is the innate immune response, in support of the adaptive immune response and in maintenance of tissue homeostasis. The established concept of the MPS has been used to unify such a diverse cell type as one functional entity.

According to this concept, monocytes developing in the bone marrow (BM) continuously colonize different tissues and mature into macrophages *in situ*. However, this concept has been challenged recently and thought to be an oversimplification. The first evidence that tissue macrophages can develop from embryonic sources and bypass monocytic intermediates came from microglia-resident macrophages in brain parenchyma. Based on the fate mapping mouse, microglia were shown to be derived from embryonic day 7.5 (E7.5) yolk sac (YS) precursors (Ginhoux et al., 2010). Furthermore, based again on fate mapping mouse, YS origin was generalized to macrophages in other tissues including epidermis, liver, spleen, lung, pancreas, and kidney (Schulz et al., 2012). In a study by Schulz et al. (2012), the authors noted that mouse tissue macrophages can consist of different pools of cells based on F4/80 and CD11b expression: F4/80^{hi} macrophages were postulated to be derived from YS precursors that are able to maintain their numbers *in situ* (resident), while CD11b^{hi} macrophages were thought to be replaced continuously by BM-generated (infiltrating) monocytes. In subsequent studies, F4/80^{hi} resident macrophages were proposed to originate from YS-derived erythro-myeloid progenitors (Gomez Perdiguero et al., 2015; Sheng et al., 2015).

Thus, the model of the MPS needs to be extended to include not just monocytes as a major source of tissue macrophages but to highlight the prenatal origins of many

populations, some of which involve cells arising from a distinct YS-embryonic macrophage lineage. The current view is that tissue-resident macrophages comprise cell populations derived from three sources: yolk sac, fetal liver and hematopoietic stem cells in the bone marrow (Fig. 1.1). The relative contributions of embryonic versus hematopoietic sources to resident macrophages vary by tissue, with some tissues being populated mainly by YS-derived macrophages (for example, Langerhans cells in the skin and microglia in the brain) and other tissues having mainly BM–derived macrophages (for example, the intestine). Another major insight has been provided by the realization that YS–derived macrophages (and presumably fetal liver–derived macrophages) can be maintained for the lifespan of the organism by continuous self-renewal. It is not yet clear whether all tissue-resident macrophages can enter the cell cycle or whether small fractions of these self-renew by asymmetric cell division (similar to stem cells). This distinction is important because of its implications for understanding the functional heterogeneity of tissue macrophages and the lack of distinct phenotypic markers able to identify unique subsets (Okabe and Medzhitov, 2015).

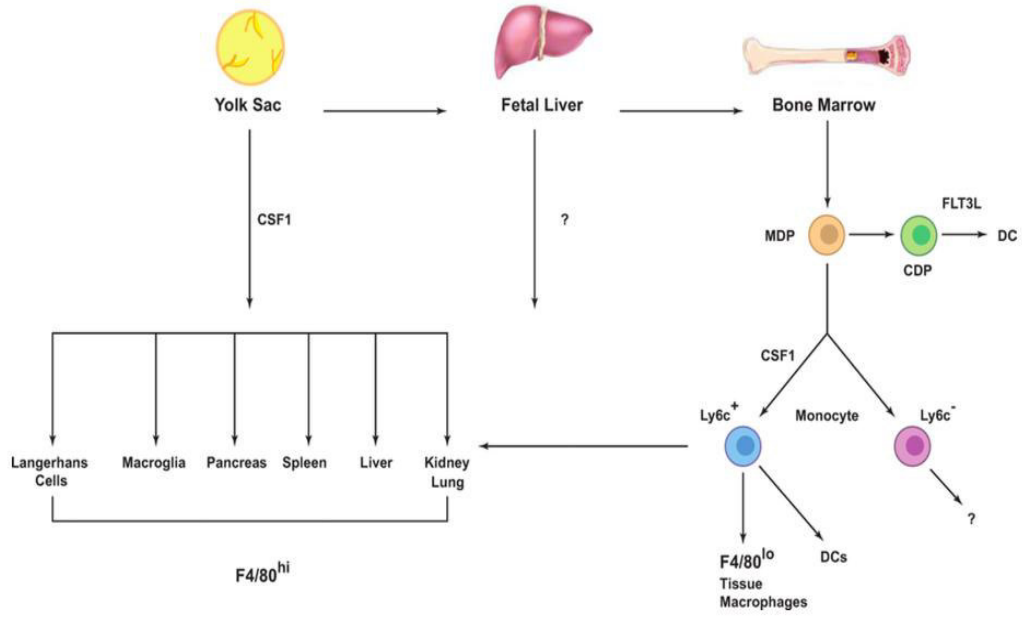

Figure 1.1: The mononuclear phagocytic system in adults derives from at least three sources. The first is the yolk sac (YS) that results in progenitors that populate all tissues and their progeny persist throughout life as F4/80 bright resident macrophages. The second from the fetal liver is less well defined but seems to contribute to adult LCs perhaps through a progenitor derived from the YS. The third lineage derives from the bone marrow (BM) to give circulating monocytes and their progeny F4/80^{low} macrophages and DCs. From Wynn et al., 2013.

A more recent idea proposed that ontogenic distinction is relevant to disease pathogenesis, as it is apparent that the functions of BM-derived monocytes can be very different from those of tissue-resident macrophages in the same inflammatory environment. The two cell types have distinct expansion mechanisms and distinct functions in the brain during experimental autoimmune encephalitis. Infiltrating monocytes are recruited via extravasation from blood vessels and produce inflammatory mediators important for disease progression but do not persist after the resolution of inflammation. In contrast, activated resident microglia cells proliferate locally, persist and return to quiescence following remission. Thus, it might be inaccurate to describe tissue-resident macrophages as always being 'anti-inflammatory' in contrast to passenger macrophages that are always 'pro-inflammatory'. A connection between ontogenesis and function could be possible but the respective roles of tissue-resident macrophages and passenger macrophages remain to be studied in detail, characterizing the underlying molecular mechanisms involved (Gomez Perdiguero and Geissmann, 2015).

1.2.1 Monocyte heterogeneity

Monocytes are a critical part of the MPS and are involved in many diseases with an inflammatory component, such as infection, cardiovascular disease, type-1 diabetes and cancer. Blood monocytes represent a large pool of scavenger and potential effector cells inside blood vessels in homeostasis as well as during inflammatory processes. In mammals, monocytes also represent accessory cells, which can link inflammation and the innate defense against microorganisms to adaptive immune responses. Indeed, the best known function of monocytes is as a considerable systemic reservoir of myeloid precursors for the renewal of some tissue macrophages and antigen-presenting DCs (Auffray et al., 2009). Several lines of evidence have indicated that the role of monocytes, both in the control of pathogens and in the pathophysiology of inflammation, can be attributed to different functional groups. Therefore, the issue of heterogeneity of monocytes becomes relevant for human health. Monocytes are equipped with a large array of scavenger receptors that recognize microorganisms but also lipids and dying cells,

and stimulated monocytes can produce large quantities of effector molecules, such as reactive oxygen species (ROS), prostaglandins, cytokines including tumor necrosis factor (TNF)-α, interleukin (IL)-1β, IL-8, IL-6 and IL-10, vascular endothelial growth factor (VEGF), and proteolytic enzymes involved in the defense against pathogens and in the pathogenesis of several inflammatory diseases, including arthritis and atherosclerosis. Although the heterogeneity of monocytes is not fully understood, one theory suggests that monocytes continue to grow and mature into the blood and tissues, and can be recruited at different stages during the maturation process (Fig. 1.2). The state of maturation at the time they leave the blood stream can, in fact, define their function.

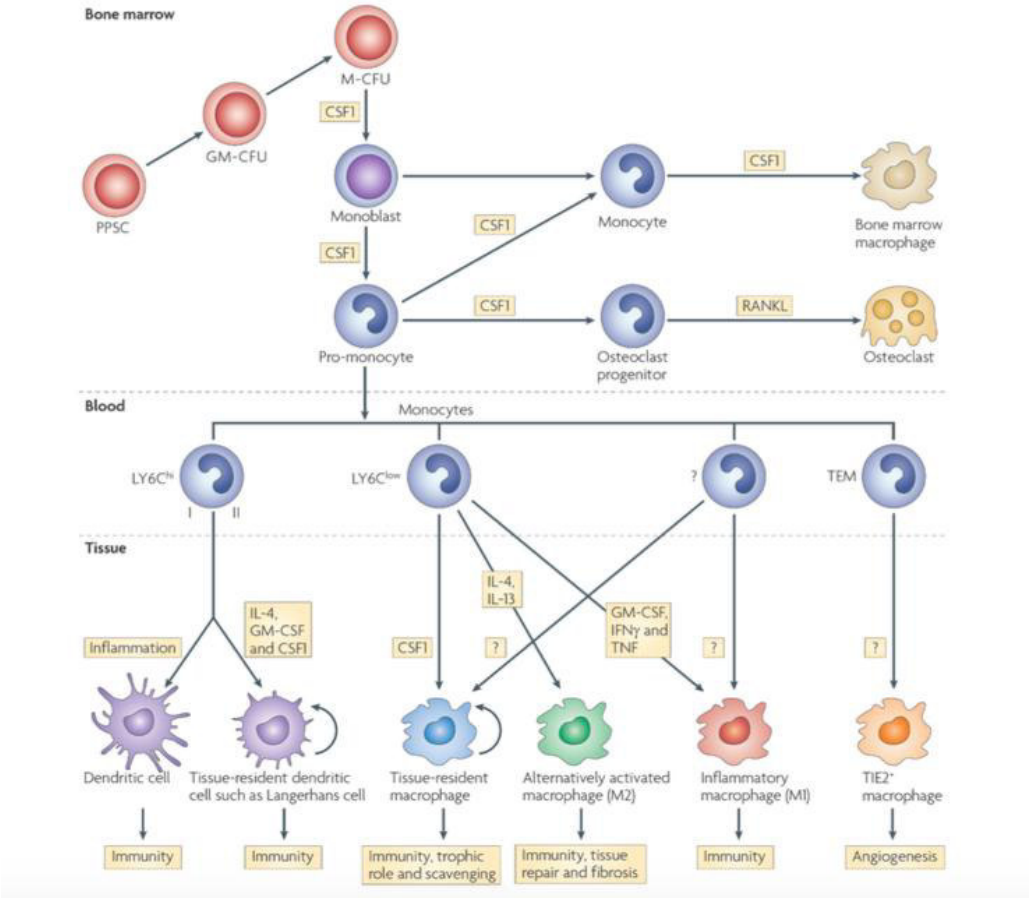

Figure 1.2: Cells of the mononuclear phagocytic system (MPS) arise in the bone marrow, where they develop from pluripotent stem cells (PPSCs) through various multipotent progenitor stages: granulocyte/macrophage colony-forming unit (GM-CFU) to macrophage CFU (M-CFU) to monoblast to pro-monocyte. In the bone, osteoclast progenitors develop from these cells under the influence of colony-stimulating factor 1 (CSF1), and these differentiate in response to receptor activator of nuclear factor-κB ligand (RANKL) into osteoclasts. Another population differentiates into bone marrow macrophages also in response to CSF1, and the *ex vivo* culture of these cells and their progenitors is often used for macrophage studies. In addition, monocytes are released into the circulation. From Pollard et al., 2009.

The existence of at least two phenotypically and functionally distinct monocyte subsets has been demonstrated in humans and mice, which suggests evolutionary conservation of monocyte heterogeneity (Gautier et al., 2009). Monocytes represent about 10% of leukocytes in human blood and 4% of leukocytes in mouse blood. Studies examining homing and differentiation of mouse monocytes *in vivo* have identified two major monocyte subpopulations based on their expression profile of the surface marker Ly6C (or GR-1), and chemokine receptors such as CCR2 (CCL2 chemokine receptor) and CX3CR1 (CX3C chemokine receptor 1, also known as fractalkine receptor; Hristov and Weber, 2011). Ly6C is a useful marker to distinguish different populations of murine monocytes and macrophages: it belongs to a family of cell surface phosphatidylinositol-anchored glycoproteins expressed in varying degree in leukocytes, although its function remains unknown (Brancato and Albina, 2011; Motwani and Gilroy, 2015). Inflammatory monocytes, characterized as $Ly6C^{high}/CX3CR1^{low}/CCR2^{+}$ cells, migrate into sites of inflammation during the early phase of the response to injury. A second population of murine monocytes, often referred to as "resident" or "patrolling", are defined as $Ly6C^{low}$ $CX3CR1^{hi}/CCR2^{-}$ cells, which egress the circulation into wounds and other sites of inflammation to resolve the immune response (Hristov and Weber, 2011; Ginhoux and Jung, 2014). In mice, classical and non-classical monocyte frequency is approximately 1:1 (Fig. 1.3).

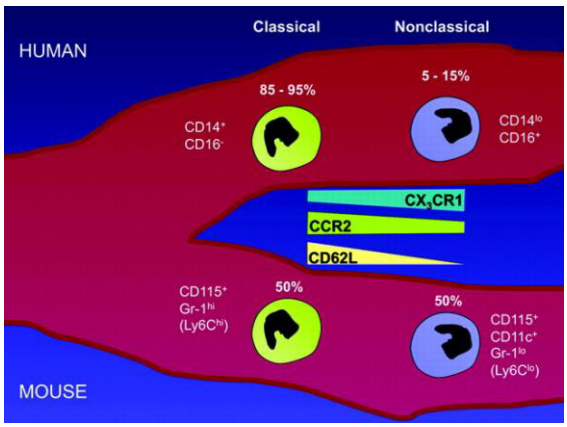

Figure 1.3: Circulating monocyte heterogeneity. Peripheral blood circulating monocytes are present in two distinct populations, called "classical" and "non-classical" with different relative abundance (expressed in %) and characterized by different pattern of surface markers. This classification has been demonstrated both in mice (lower portion of the image) and in humans (upper portion). From Gautier et al., 2009.

In humans, monocytes were initially identified by their expression of large amounts of CD14 (a cluster of differentiation which is part of the lipopolysaccharide receptor). However, the subsequent identification of differential expression of antigenic markers showed that monocytes in human peripheral blood are heterogeneous, and this provided the first clues to the differential physiological activities of monocyte subsets. Differential expression of CD14 and CD16 (also known as FCγRIII) allowed human monocytes to be distinguished into two separate subsets, similar to monocyte classification in mice: as depicted in Fig. 3, $CD14^{hi}/CD16^{-}$ cells, which are often called classical monocytes, represent 80% to 90% of circulating monocytes and express high levels of the chemokine receptor CCR2 and low levels of CX3CR1. Conversely, $CD14^{low}/CD16^{+}$ cells, or non-classical monocytes, have a $CX3CR1^{high}/CCR2^{low}$ phenotype (Gordon and Taylor, 2005; Mantovani et al., 2009; Ziegler-Heitbrock et al., 2010).

1.2.2 Macrophage plasticity and polarization

A key feature of macrophages is their ability to 'tailor' their responses according to environmental stimuli. Upon encountering pathogens, macrophages express pro-inflammatory cytokines and reactive oxygen and nitrogen species that aid antimicrobial and immune activation functions needed to kill and control pathogens. By contrast, homeostatic signals induce macrophages to adopt phenotypes linked with tissue remodeling and repair (Glass and Natoli, 2015). Because the signals encountered by macrophages are different and also dynamic, macrophages not only respond with phenotypes but also can switch from one 'functional' phenotype to another. Hence, diversity and plasticity of phenotype and function are characteristic features of macrophages (Gordon and Taylor, 2005). In macrophages, inflammatory stimuli such as lipopolysaccharide (LPS) and interferon (IFN)-γ induce an inflammatory phenotype that promotes T_H1 effector response and antimicrobial and tumoricidal properties. LPS/IFNγ activated cells are efficient producers of effectors molecules (reactive nitrogen and oxygen intermediates) and pro-inflammatory cytokines, such as IL-6, IL-1β and TNF-α, induce up-regulation of molecules associated with antigen presentation, such as major histocompatibility

complex (MHC) class II and the co-stimulatory molecules CD40, CD80 and CD86 (Mantovani et al., 2013). Macrophages with this phenotype are called 'classically activated' macrophages or M1. In contrast, stimulation of macrophages with cytokines such as IL-4 or IL-13 leads to an 'alternative' activation state or M2, characterized by low levels of inflammatory cytokines such as IL-12 and IL-23, and high levels of the anti-inflammatory cytokine IL-10, with variable capacity to produce chemokines such as CCL17, CCL18 and CCL22, and generally have high levels of scavenger, galactose-type and mannose receptors (MR or CD206). In general, IL-4/IL-13 activated cells take part in polarized T_H2 responses, parasite clearance, the dampening of inflammation, the promotion of tissue remodeling, angiogenesis, tumor progression and immunoregulation (Biswas and Mantovani, 2010).

However, macrophages in many other homeostatic or pathological situations do not show a clear M1 or M2 phenotype, or show phenotypic plasticity during disease progression, clearly indicating that the dichotomous M1-M2 model is insufficient to describe macrophage activation. In this context, Xue and collegues (2014) recently generated a resource data set to assess transcriptional regulation during human macrophage activation by comparing a diverse set of stimuli on a single microarray platform under highly standardized conditions. Network modeling of this data set allow us to extend the current M1 versus M2 polarization model to a ''spectrum model'' with distinct macrophage activation programs. Moreover, a new way of looking at macrophage activation is to consider a multidimensional model of activation, which integrates the signals to which macrophages are exposed in their specific microenvironments (Fig. 1.4; Davies and Taylor, 2015).

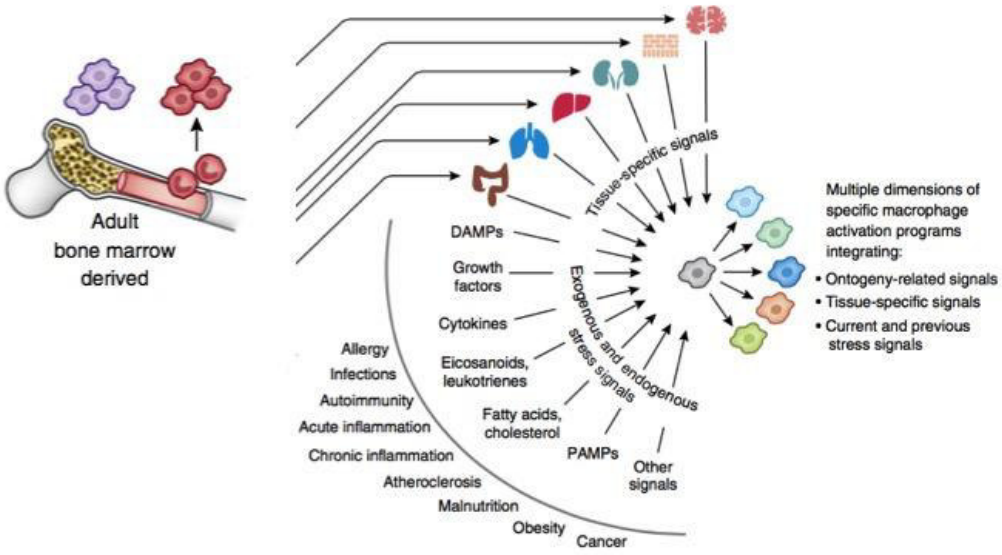

Figure 1.4: A multidimensional view of macrophage activation that is influenced by their ontogeny. Macrophages in various tissues are yolk sac derived (microglia of the brain), fetal liver monocyte derived (alveolar macrophages in the lung and Kupffer cells in the liver for example), derived from both yolk sac macrophages and fetal liver monocytes (Langerhans cells in the epidermis) or replaced after birth with adult bone marrow monocytes (gut, heart and dermal macrophages). Furthermore, tissue-specific environmental signals are important drivers of macrophage activation during adult tissue homeostasis. Once a tissue insult occurs and stress signals are elevated in the tissue environment, these new signals are further integrated in the respective program. From Ginhoux et al., 2015.

Okabe and Medzhitov (2015) in their recent review suggested that many aspects of the development and function of tissue-resident macrophages can best be described by a variation on two important factors: first, migratory progenitor cells populate different tissues, where they may receive 'tissue-identity' signals that promote their local differentiation into tissue-resident macrophages. Second, resident macrophages receive signals that indicate local functional demands, which induce diverse functional programs and associated phenotypes of macrophages, as well as their precise location and number within tissues. Thus, the phenotypes of tissue-resident macrophages are mostly a combination of differentiation and polarization programs.

In this *continuum* of plastic activation states a specific functional phenotype is associated with the expression of a wide range of particular surface proteins that can be used for macrophage identification. Unfortunately, there is diversity of

macrophage activation across species, and markers that are appropriate in mouse macrophages are not necessarily conserved in human cells (Murray et al., 2014) (Fig. 1.5). For example, in agreement with literature data, M1 macrophages can be identified by their surface expression of the scavenger receptor CD68 (a glycoprotein that binds LDL), CCR2, receptor for the chemokine CCL2 also known as MCP-1 (monocyte chemoattractant protein 1), and the co-stimulatory molecules CD80 and CD86; by contrast, M2 macrophages typically express CD163 (the scavenger receptor for the hemoglobin-haptoglobin complex), the mannose receptor CD206 (which recognizes pathogens that have mannose on their surface) and the chemokine-X3C receptor-1 (CX3CR1), also known as fractalkine receptor (Ambarus et al., 2012a; Tedesco et al., 2015).

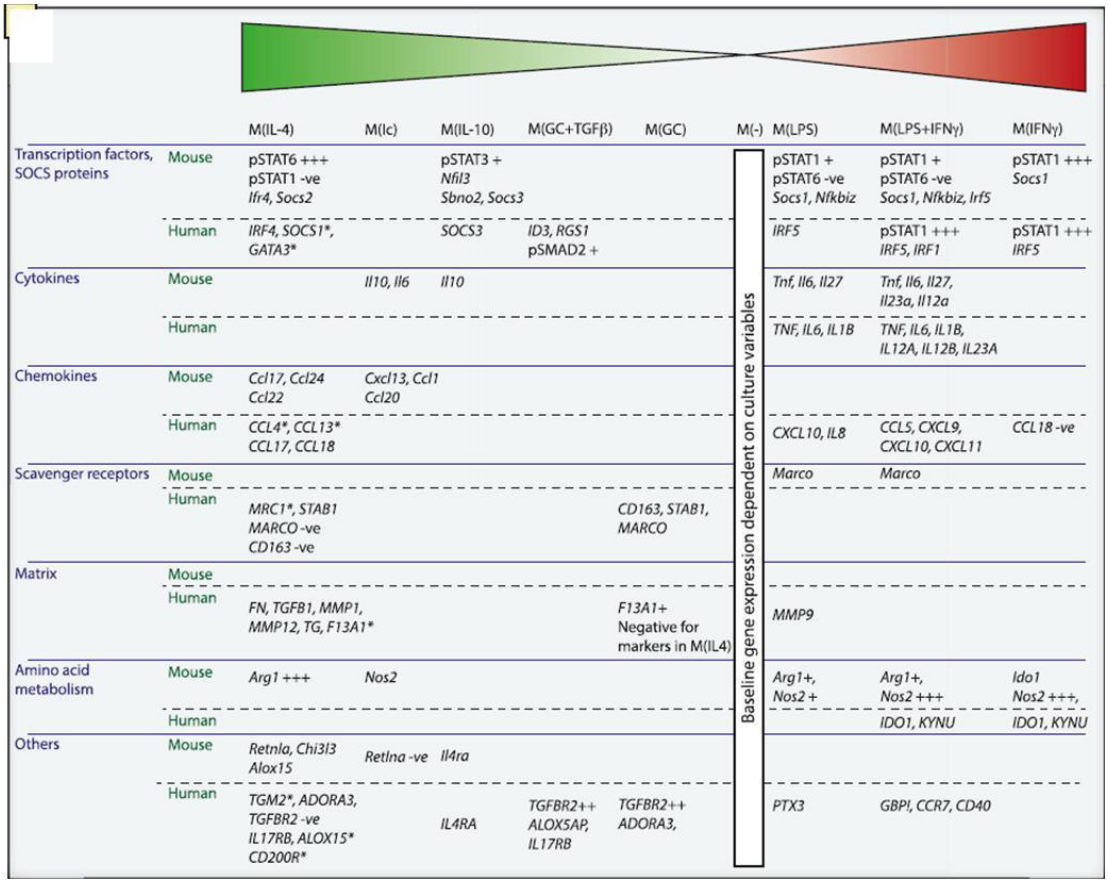

Figure 1.5: Marker systems for activated macrophages. Shown are functional subdivisions according to stimulation of mouse CSF-1 macrophages or human monocyte-derived CSF-1 macrophages with the existing M1-M2 spectrum concept. Stimulation conditions are IL-4, immune complexes (Ic), IL-10, glucocorticoids (GC) with transforming growth factor β (TGF-β), glucocorticoids alone, LPS, LPS and IFNγ, and IFNγ alone. Marker data were drawn from a wide range of published and unpublished data from the authors' laboratories and represent a starting consensus. An asterisk indicates corroboration of human IL-4 genes by deep sequencing. From Murray et al., 2014.

In vitro activation of monocyte-derived macrophages using cytokines, growth factors, prostaglandins, glucocorticoids and toll-like receptor (TLR) agonists, alone or in combination, represents a potential therapeutic approach to prevent the development of disease and promote immune tolerance in mice and humans.

1.3. ROLE OF M1 AND M2 MACROPHAEGS IN CHRONIC INFLAMMATORY DISEASES

Macrophages are central to tissue development, homeostasis and inflammation, but they also contribute to a broad spectrum of inflammatory pathologies and thus represent key therapeutic targets (Ginhoux et al., 2015). The dynamic balance between M1 and M2 phenotypes requires a fine regulation, otherwise the resulting loss of immune regulation contributes to the development and/or exacerbation of chronic inflammatory diseases, such as atherosclerosis (Pello et al., 2011; Chinetti-Gbauguidi et al., 2015), rheumatoid arthritis, obesity (Kammoun et al., 2014) and insulin resistance (Fig. 1.6; Fadini et al., 2013). This occurs with combined deficits in the number and/or function of multiple types of regulatory cells leading to the inability to sustain M2 macrophages. Although what causes these immunoregulatory mechanisms to fail is unknown, inappropriate stimulation of pro-inflammatory cells could be one of the inciting events for chronic systemic inflammation (Han and Levings, 2013).

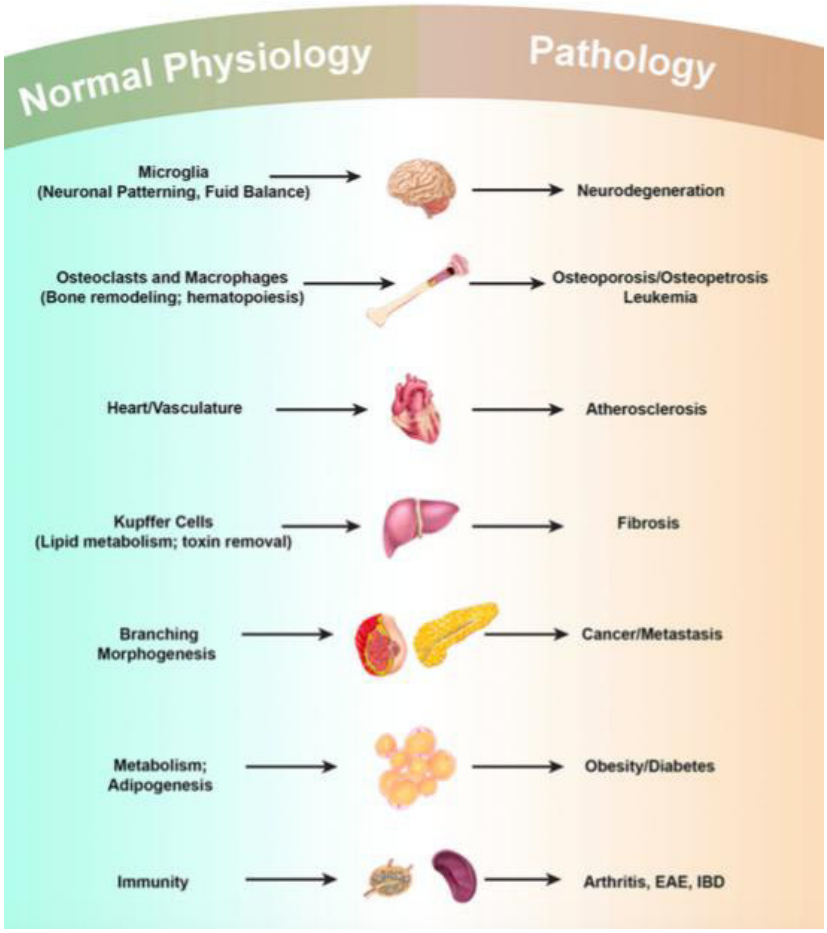

Figure 1.6: Macrophages play many developmental roles shaping the architecture of tissues ranging from the brain to bone to the mammary gland. Once development is over, macrophages modulate homeostasis and normal physiology through regulating diverse activities including metabolism and neural connectivity and by detecting damage. These trophic and regulatory roles, however, are often subverted by continuous insult and macrophages contribute to many diseases that are often associated with aging. From Wynn et al., 2013.

1.3.1 Atherosclerosis

Macrophage accumulation within the vascular wall is a hallmark of atherosclerosis. In atherosclerotic lesions, macrophages respond to various environmental stimuli, such as modified lipids, cytokines, and senescent erythrocytes, which can modify their functional phenotypes. In particular, the disease is characterized by intimal lesions of the vessel wall, and a switch from M2 to M1 macrophage phenotype has been hypothesized to occur during atherogenesis, similarly to what happens in obese subjects. Indeed, macrophages are involved in all key stages of atherosclerosis development including early inflammatory injury, development of

fatty streaks and finally plaque rupture. Several studies on human atherosclerotic plaques demonstrate that the relative proportions of macrophage subsets within a plaque might be an indicator of plaque phenotype and stability (Chinetti-Gbauguidi et al., 2015). During the development and progression of atherosclerosis, macrophages are exposed to many different environmental cues, including pro- and anti-inflammatory cytokines, cholesterol, oxidized lipids, and heme that influence gene expression and regulate macrophage function (Leitinger and Schulman, 2013). Cholesterol crystals for example, found in advanced atherosclerotic lesions, were recently shown to be also present at early stages of atherosclerotic lesions. In LPS-primed human peripheral blood mononuclear cells and *in vivo* in mice, cholesterol crystals activate the caspase-1-activating-NLRP3 inflammasome, thus inducing the cleavage and the release of IL-1 family cytokines (including IL-1β and IL-18; Duewell et al., 2010). This observation suggests that cholesterol crystals act as a M1 pro-inflammatory *stimulus* (Colin et al., 2014). Another important event acting in the atherosclerotic lesions is the rupture of microvessels that releases erythrocytes, which can be phagocytosed by macrophages, leading to an increase in iron content and release of heme associated with oxidized lipid deposition. Hemoglobin-stimulated macrophages are characterized by high levels of CD206 and CD163 and by the secretion of anti-inflammatory cytokines, such as IL-10 (Chinetti-Gbauguidi et al., 2015). Other factors, such as cytokines, senescent cells and growth factors that are present in the plaque, can influence macrophages activation.

Besides the total number of macrophages, histological analysis revealed a specific spatial distribution of distinct macrophage subpopulations in human atherosclerotic plaques (Fig. 1.7). In the human plaque shoulder, the site most prone to plaque rupture, M1 macrophages represent the principal population, while the repartition of M1/M2 macrophages is similar in fibrous cap regions. Thus, potential deleterious effects of M1 macrophages may be counteracted by protective pro-fibrotic and tissue repair effects of M2 macrophages in the fibrous cap, while the limited number of M2 macrophages cannot balance the M1-mediated effects in the plaque shoulder. Interestingly, M2 macrophages are the predominant population in the adventitia of the human atherosclerotic plaque, suggesting that these M2

macrophages may have migrated from the surrounding perivascular adipose tissue (Colin et al., 2014).

The identification of biological stimuli that can modulate macrophages activation could lead to the development of novel therapeutic approaches for the treatment of atherosclerosis (Chinetti-Gbauguidi et al., 2015).

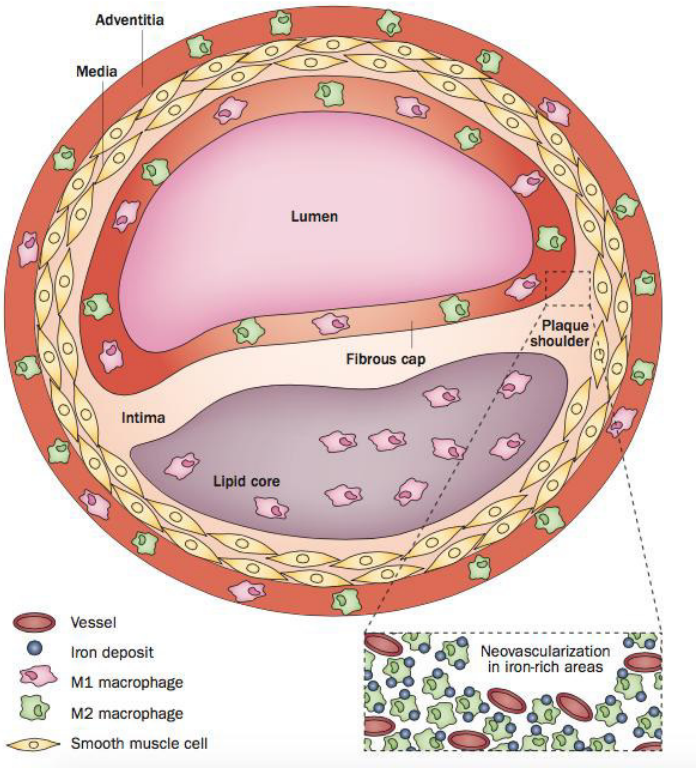

Figure 1.7: Localization of macrophage subsets in human atherosclerotic lesions. M1 macrophages are predominantly found in the plaque shoulder and lipid core, whereas M2 macrophages are most abundant in the adventitia and areas of neovascularization, which also contain iron deposits. Fibrous caps contain similar amounts of both macrophage subsets. From Chinetti-Gbauguidi et al., 2015.

1.3.2 Obesity and type-2 diabetes

Obesity-associated adipose tissue inflammation appears to be caused by infiltration of inflammatory immune cells and a parallel loss or functional reprogramming of immunoregulatory cells. Together, these changes lead to a variety of positive feedback pathways that not only sustain chronic inflammation, but also contribute to the development of insulin resistance and type-2 diabetes. The key point is that

the inflammation accompanying obesity is distinctly different to that of acute inflammation, as the inflammatory *stimulus* fails to be resolved (Kammoun et al., 2014). The general view in obesity is that there is an imbalance in the ratio of M1/M2 macrophages, with pro-inflammatory macrophages being enhanced compared with anti-inflammatory macrophages being down-regulated, leading to chronic inflammation and the propagation of metabolic dysfunction. In a healthy state M2 macrophages are induced by peroxisome proliferator activated receptor (PPAR)-γ signaling and maintain adipocyte function, insulin sensitivity and glucose tolerance, which can prevent the development of diet-induced obesity and type-2 diabetes (Murray and Wynn, 2011). However, weight gain induces local inflammation and chemokine production to promote recruitment of circulating pro-inflammatory ($Ly6C^{hi}$) monocytes. Recruited monocytes differentiate into an M1 macrophage phenotype and their accumulation leads to an imbalance between M1 and M2 macrophages. Increased cytokine production from M1 macrophages and/or reduced anti-inflammatory signals from the M2 macrophages promotes adipose tissue dysfunction and impairs glucose tolerance (Fig. 1.8; Kraakman et al., 2014).

Evidence for the detrimental role of M1 macrophages in promoting adipose tissue insulin resistance is accumulating. A recent study on novel phenotypes of blood monocytes shows that type-2 diabetes is also associated with a marked reduction of the anti-inflammatory M2 phenotype. Fadini and colleagues (2013) found that hypercholesterolemia and type-2 diabetes are characterized by a marked reduction in M2 cells while M1 cells are unchanged compared with controls; as a result, the M1/M2 polarization ratio is increased in diabetes. As type-2 diabetes is considered a pro-inflammatory condition, it is striking that the monocyte polarization imbalance is attributable to a defect in anti-inflammatory rather than an excess of pro-inflammatory cells (Fadini et al., 2013). This observation is in line, however, with the view that diabetes is a disease of impaired damage control (Schaper and Havekes, 2012), in which injury is worsened by defective repair.

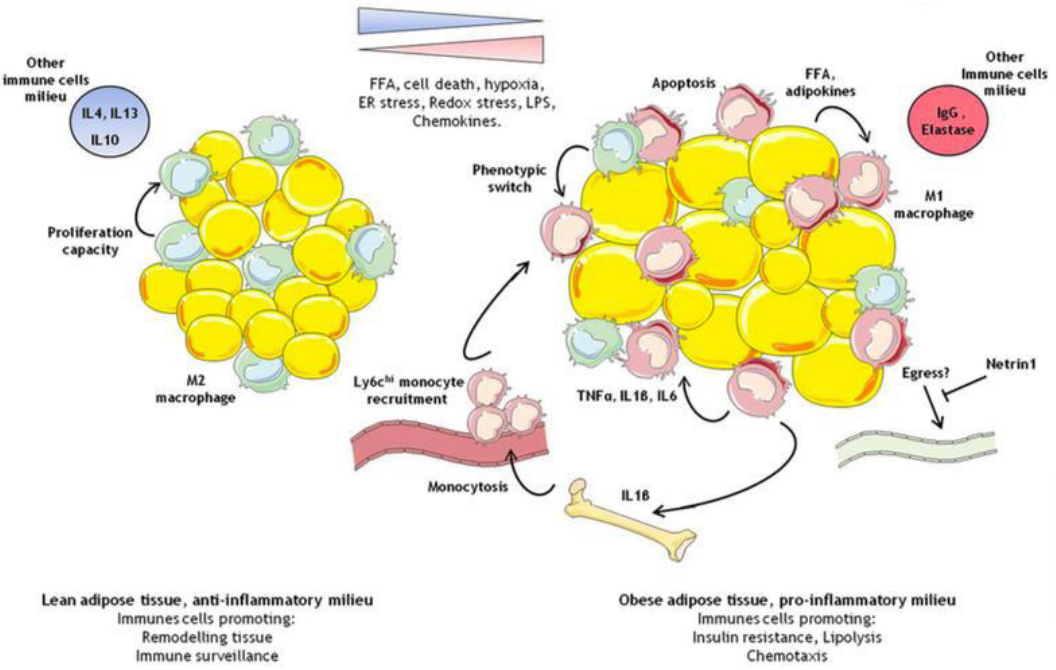

Figure 1.8: In the lean healthy adipose tissue, M2 like macrophages self-maintain through proliferation. They ensure tissue remodeling and pathogen screening. In the obese adipose tissue, over nutrition leads to larger adipocytes, which coupled with cellular stress, and promotes the development of a pro-inflammatory environment. In this context, M1-like macrophages start to accumulate. From Kraakman et al., 2014.

1.4. *IN VITRO* MODELS OF MACROPHAGE ACTIVATION

Macrophages, derived from monocyte precursors, undergo specific differentiation depending on the local tissue environment. The various macrophage functions are linked to the type of receptor interaction on the macrophage surface and, crucially, to the cytokine *milieu* in the microenvironment (Ginhoux and Jung, 2014). Human monocytes can be obtained from three different main sources: whole blood, cord blood, or the human monocyte cell line THP-1. Cord blood monocytes are selected as $CD14^+$ from the mononuclear stem cells (Jaatinen and Laine, 2007). Conversely, THP-1 cells are derived from human acute monocytic leukemia and can be differentiated to macrophages by adding phorbol ester (TPA) into the culture medium (Tjiu et al., 2009). The most commonly used are circulating monocytes that can be obtained following different approaches; the isolation process of mononuclear cells from whole blood affects the subsequent differentiation method to obtain mature macrophages. Peripheral blood mononuclear cells (PBMCs) can be

isolated from whole blood samples by density gradient centrifugation, for example using Ficoll-Paque^{TM}, a polymer that stratifies the different blood components according to their specific weight. Then PBMCs can be stratified upon hyper-osmotic Percoll (another synthetic polymer), and pure monocytes are obtained after a second gradient centrifugation. With this method monocyte purity is 95-98% (Repnik et al., 2003). Alternatively, purified monocytes can be obtained through magnetic cell sorting using specific CD14-labeled magnetic beads (Bender et al., 2004; Martinez et al., 2013). This method usually allows obtaining a 90% monocyte ($CD14^+$) pure suspension. Working with highly pure monocytes population requires exogenous growth factors and/or cytokines (i.e. colony-stimulating factor-1 (CSF-1) or granulocyte macrophages colony-stimulating factor (GM-CSF)) in the culture medium for survival of monocytes (Jaguin et al., 2013).

Nature of polarizing agents and exposure time appear to be crucial, especially when testing the potential impact of pharmacological interventions. For this reason a panel of experts published experimental guidelines for macrophage activation and polarization (Murray et al., 2014), trying to clarify something that in literature is very contentious and confusing. If seeded after Ficoll separation, human monocyte-derived macrophages are able to spontaneously differentiate *in vitro* in the absence of growth factors other than those contained in animal or human serum (Ambarus et al., 2012a; Eligini et al., 2013; Tedesco et al., 2015). Spontaneous macrophage differentiation may be related to the relative abundance of T_H2 cytokines secreted by $CD3^+$ lymphocytes early in culture before their detachment and/or by the fraction of lymphocytes which could be persistent in culture during the whole differentiation period. By contrast, working with pure monocyte populations (using Percoll-or beads-based methods) requires differentiation stimuli like CSF-1 or GM-CSF. There is no compelling evidence that these two factors could influence the subsequent macrophages activation (Murray et al., 2014). It is also important to define the mediators, used alone or in various combination, that are used for the generation of activated macrophages. Furthermore, Murray et al. proposed that researchers describe also stimulation scenarios and adopt a nomenclature linked to the activation standards (i.e. M(LPS) or M(IL-4)). Developing gold standard

differentiation/activation protocols would be useful to compare data from different research groups and perform screens of macrophage activation-modifying pharmacological agents.

1.5. PHARMACOLOGICAL CONTROL OF MACROPHAGE POLARIZATION

Specific macrophage-target therapies are now taking the first steps into clinical investigations. In addition, therapeutic approaches not originally designed as macrophage oriented or specific have been found to affect macrophage activation and polarization (Sica and Mantovani, 2012). Therefore, it is relevant to identify novel mechanisms for the pharmacological control of human macrophage polarization. For instance, although it is well established that glucocorticoids induce multiple effects on several immune cell types, glucocorticoid treatment of human monocytes does not cause a global suppression of monocytic effector functions but rather results in differentiation of a specific anti-inflammatory phenotype which seems to be involved in resolution of inflammation (Ehrchen et al., 2007). Similarly, Vallelian et al. (2010) found that glucocorticoid treatment of monocytes *in vitro* and in patients on glucocorticoid-pulse therapy polarizes monocytes into a M2/alternatively activated phenotype with high Hb-scavenger receptor (CD163) expression and enhanced Hb clearance and detoxification. A positive regulation of CD163 following dexamethasone treatment was demonstrated in recent studies in human macrophages (Ambarus et al., 2012a; Tedesco et al., 2015). Opposite effects on macrophage polarization were observed on human monocyte-derived macrophages challenged with the immunosuppressant agent rapamycin after polarization. The presence of rapamycin induces apoptosis in M2 but not in M1 macrophages, and enhances M1 surface markers and pro-inflammatory cytokines production together with a reduction of typical M2 markers (Mercalli et al., 2013). Statins are thought to reduce vascular inflammation through lipid-independent mechanism. Van der Meij et al. (2013) evaluated the anti-inflammatory potency of simvastatin and atorvastatin in patients on therapy for at least 6 weeks. Both statins equally effectively and dose-dependently shifted macrophage polarization towards

a M2 phenotype and reduced vascular wall nuclear factor kappa-light-chain-enhancer of activated B cells (NF-κB) activity in abdominal aorta aneurysms samples, thus diminishing inflammatory responses. The inhibition of the NF-κB pathway was demonstrated also in monocytes treated *in vitro* with rosuvastatin (Margaritis et al., 2014). PPARγ agonists (thiazolidindiones) have long been used in the treatment of diabetes. The evidence linking PPARγ to M2 polarization provides new insights into their mode of action. It has been demonstrated that rosiglitazone markedly increases the number of macrophages in adipose tissue of obesity-induced mice. In particular, markers for classically activated macrophages including IL-18 are down-regulated, whereas markers characteristic for alternatively activated macrophages (arginase 1, IL-10) are up-regulated by rosiglitazone (Stienstra et al., 2008). Interestingly, a positive correlation between the expression of M2 markers and PPARγ has been shown in human atherosclerotic lesions. Moreover, PPARγ activation primes primary human monocytes into alternative M2 macrophages with anti-inflammatory properties (Bouhlel et al., 2007).

New insights come from microRNA (miRNA) studies. miRNAs have recently emerged as a major class of gene expression regulators linked to most biological functions. In particular, the miRNA let-7c, which is overexpressed in M2 compared with M1 subset of mouse bone marrow-derived macrophages, plays an important role in regulating macrophage polarization (Banerjee et al., 2013). Furthermore, a procedure for generating pharmaceutical-grade human regulatory macrophages has been recently developed and approved for a clinical trial as an adjunct immunosuppressive agent in living-donor kidney transplantation (clinicaltrials.gov: NCT02085629). To date, two patients have been treated with human regulatory macrophages preparations, both of whom have not undergone any rejection episode after more than 6 years after transplantation (Hutchinson et al., 2011).

Therefore, several medications appear to have an impact on the functional status of macrophages; however, the extent to which their effect on macrophages explains their clinical efficacy remains to be defined. The identification of mechanisms and molecules associated with macrophage plasticity and polarized activation provides a basis for macrophage-centered diagnostic and therapeutic strategies.

In the next section a short account is provided on the potential of novel analogues of natural compounds to modulate human macrophage activation and polarization. In particular, although anti-inflammatory effects of curcumin have been reported in a variety of experimental models (Aggarwal and Harikumar, 2009; Shehzad et al., 2013), the possibility that curcumin and/or analogues thereof affect human macrophage activation has not been explored in much detail.

1.6. CURCUMIN

Turmeric (*haldi*), a rhizome of *Curcuma longa*, is a flavorful yellow-orange spice. Its plant is 1 meter in height and has lance-shaped leaves and spikes of yellow flowers that grow in a fleshy rhizome or in underground stem. An orange pulp contained inside the rhizome constitutes the source of turmeric medicinal powder (Nagpal and Sood, 2013). Curcumin (1,7-bis(hydroxyl-3-methoxyphenyl)-1,6-heptadiene-3,5-dione) is the most important active polyphenolic ingredient responsible for the biological activity of turmeric. It was first isolated from the drug in 1815 by Vogel and Pelletier, but its structure was not elucidated until 1913 (Fig. 1.9). Curcumin is insoluble in water, but soluble in ethanol and acetone. Components of tumeric are named curcuminoids and the naturally occurring ratios of curcuminoids in curcumin are about 5% bisdemethoxy curcumin, 15% demethoxy curcumin, and 80% curcumin. The various components of the turmeric have their medical importance (Alok et al., 2015). Curcumin has been used extensively in ayurvedic medicine for centuries and various pharmacological actions of curcumin have been investigated by researchers worldwide, as it appears to be nontoxic and shows a variety of possible therapeutic indications (Nagpal and Sood, 2013; Ghosh et al., 2015).

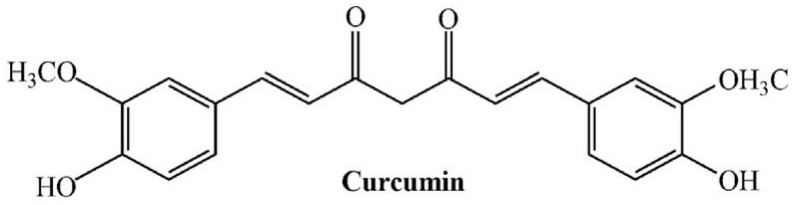

Figure 1.9: The chemical structure of curcumin, first described by Milobedzka et al. in 1910

The wound healing potential of curcumin is attributed to biochemical effects such as its anti-inflammatory, anti-infectious and anti-oxidant activities (Akbik et al., 2014), but the mechanisms of action of this natural compound will be discuss more in details in Section 7 below.

1.6.1 Curcumin analogues

Poor bioavailability, rapid metabolism and adverse effects observed in some studies are major problems that limited curcumin clinical investigation and application (Maheshwari et al., 2006; Anand et al., 2008). For this reason, in the present work we decided to assess the pharmacological profile of two additional curcumin-based analogues, called GG6 and GG9. The molecular structures of GG6 and GG9 are shown in Fig. 1.10. The aim of designing and synthetizing a library of curcumin-based analogues is to perform a structure-activity relationship study and to determine the essential chemical features required to modulate the selected targets involved in inflammatory processes and diseases (i.e. TLR-4 activation). To this end, the aryl side rings of this scaffold was decorated with selected substituents and modifications were performed on the central α, β-unsaturated carbonyl fragment in order to assess its importance for biological activity. Published synthetic procedures for curcumin derivatives include the Pabon reaction, in which selected aldehydes were reacted with 2,4-pentanedione under well-defined reaction condition (Pabon, 1964). This procedure proved to be suitable for a parallel chemical synthesis approach, which allows one to obtain libraries of analogues. In particular, the commercial availability of large numbers of synthetic intermediates (aldehydes and acetophenones) permitted the incorporation of a broad chemical diversity for the newly synthetized molecules.

GG6

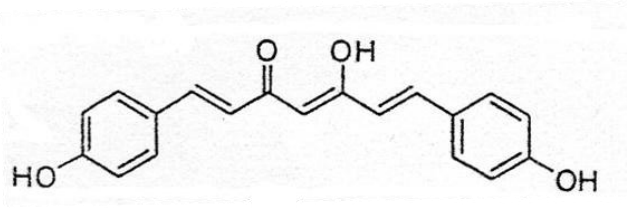

GG9

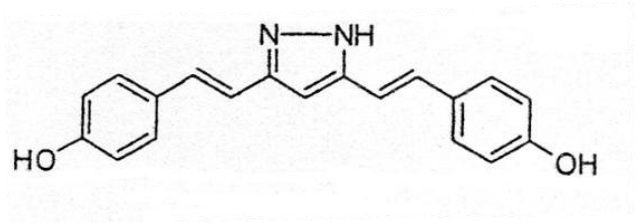

Figure 1.10: Molecular structure of synthetic curcumin-based anaogues GG6 and GG9. These molecules were kindly provided by Prof. Federica Belluti (University of Bologna).

1.7. CURCUMIN AND THE IMMUNE SYSTEM

Curcumin has been used for its various therapeutic properties for thousands of years. It is clear from various studies that curcumin, like many natural products, has many biological activities and is relatively safe and well-tolerated. It is also nontoxic even at doses up to 8 g per day. The effects of curcumin are mediated partially through its antioxidant and anti-inflammatory properties. At the same time it can also modulate multiple signaling molecules like transcription factors, enzymes and secondary messengers, thereby controlling expression of many genes, and is potentially effective in the case of many disease conditions associated with impaired regulation of such signaling pathways (Fig. 1.11; Ghosh et al., 2015).

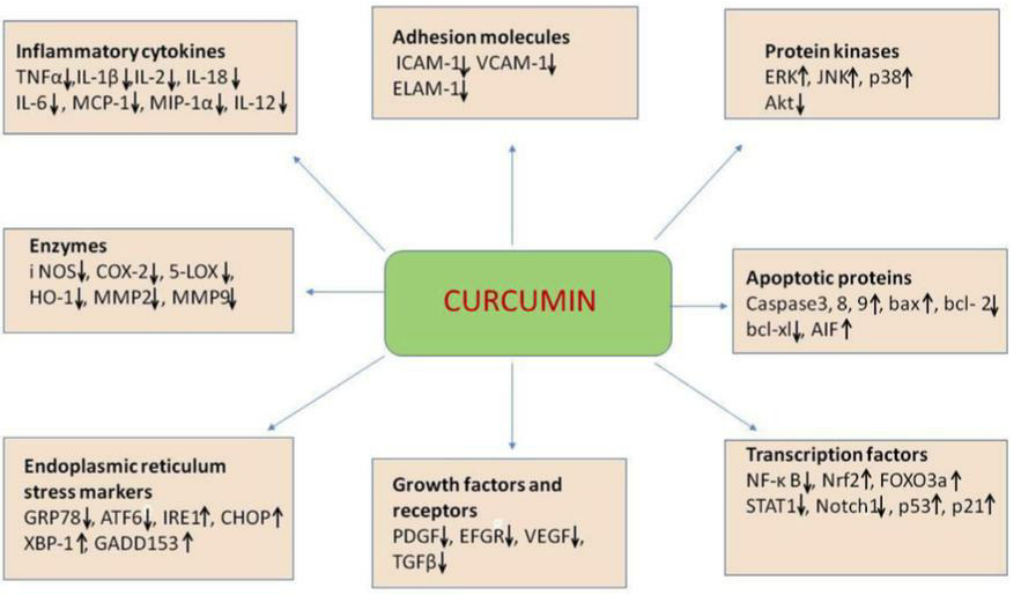

Figure 1.11: Various cellular signaling molecules modulated by curcumin. From Ghosh et al., 2015.

With regard to the physicochemical and antioxidant activities of curcumin, the keto-enol-enolate equilibrium of the heptadienone moiety has been reported to be essential (Tocharus et al., 2012). The central CH_2 group adjacent to the highly activated carbon atom in the heptadienone link may be the actual reaction site because the C-H bonds on this carbon should be very weak due to massive delocalization of the unpaired electron on the adjacent oxygen atoms. Besides, the phenolic OH is the most preferable group for the proton loss from the one-electron oxidized species. As the resultant phenoxyl radical is stabilized by delocalization of electrons, the ability for curcumin to scavenge the oxidizing free radicals is greatly increased. The resonance-stabilized radicals can undergo further loss of the second hydrogen atom from the second phenolic OH group, producing a diradical. This diradical may be converted into stable products like quinones or undergo cleavage to produce smaller phenols like ferulic acid. The theoretical data on atomic charge and the bond energy calculation for H atom dissociation channel from various sites of curcumin and its radicals do support the experimental observations (Priyadarsini et al., 2003; Menon and Sudherr, 2007; Ghosh et al., 2015).

Curcumin is a well-known anti-inflammatory agent. Joe et al. (2004) thoroughly reviewed the numerous mechanisms by which curcumin modulates inflammation.

Most notably, curcumin was shown to inhibit the production of TNF-α and IL-1β, two main cytokines released from monocytes and macrophages that play important roles in the regulation of inflammatory responses. The natural compound modulates TNF-α expression by affecting the methylation pattern of TNF-α promoter (Reuter et al., 2011), activating Nrf2/HO-1 and down-regulating the expression of TNF-α, IL-1β, IL-6 and IL-8 (Priyanka et al., 2014; Liu et al., 2015). Of equal importance is curcumin's ability to inhibit the activity of NF-κB, a transcriptional factor that regulates many genes involved in the initiation of inflammatory responses. NF-κB is normally activated by various kinases (AKT, PI3K, IKK), and curcumin affects various pathways implicated in its activation, as shown in Fig. 1.12 (Akbik et al., 2014).

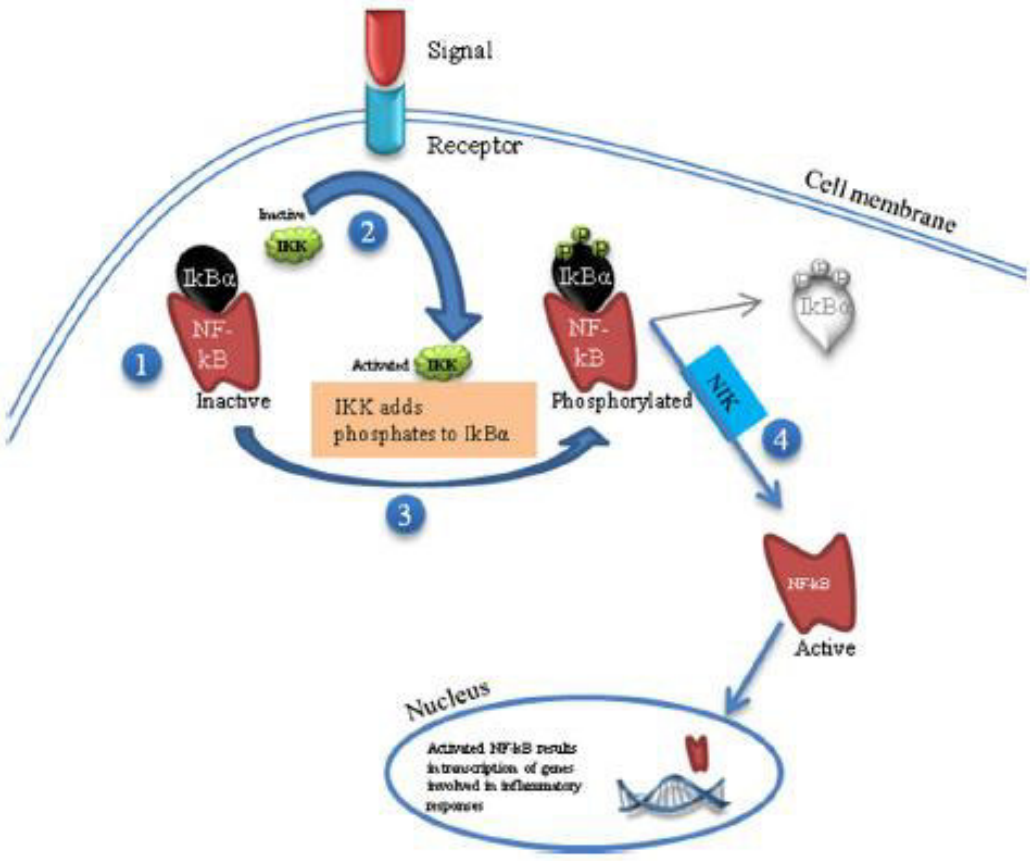

Figure 1.12: Curcumin interferes with inflammatory pathways by blocking the transcription factor NF-κB. The numbers 1, 2 and 3 represent the pathways inhibited by curcumin. From Aknik et al., 2014.

With regard to NF-κB receptor-dependent activation, Youn et al. (2006) described the inhibition of TLR4 homodimerization by curcumin. Activation of TLRs, a major family of pattern recognition receptors, provides an important step by which immune cells initiate inflammatory response through recognizing both invading pathogens and endogenous danger signals (Lien and Golenbock, 2003). In particular, TLR4, in association with its co-receptor myeloid differentiation protein-2 (MD-2), is responsible for the recognition of LPS, the major Gram-negative bacteria wall component, and represents a primary mediator of immune response. LPS induces the activation of NF-κB through both MyD88- and TRIF-dependent pathways, and the activation of IRF3 through TRIF-dependent pathway. Curcumin inhibits LPS-induced NF-κB and IRF3 activation in RAW264.7 cells (Youn et al., 2006). Furthermore, curcumin has been shown to suppress the activation of NF-κB induced by various pro-inflammatory stimuli by inhibiting IKKβ kinase activity (Jobin et al., 1999), suggesting that the molecular targets of curcumin include the TLR4 receptor complex in addition to IKKβ. Youn et al. described in more detail the molecular mechanisms by which curcumin acts on NF-κB pathway: the compound inhibits the dimerization of TLR4 induced by LPS, and its α,β-unsaturated carbonyl group can react with –SH group in cysteine in the activation loop of IKKβ, inhibiting the kinase activity of IKKβ (Youn et al., 2006). More recently, Zhou et al. (2015) confirmed these data. Therefore, the main effect of curcumin appears to be on LPS activation, especially on the expression of M1 markers (such as CD80) that are modulated through the NF-κB pathway (Lien and Golembock, 2003).

In the literature curcumin is also reported to affect M2 activation: in particular, one study showed that curcumin could not only directly induce the polarization of macrophages to M2 phenotype, but also promote conversion of macrophages from M1 to M2 phenotype (Chen et al., 2014). More recently, Gao et al. (2015) demonstrated that curcumin induces macrophage M2 polarization by increasing the production of IL-4 and/or IL-13 in a STAT6-dependent manner. They also observed that curcumin attenuates experimental autoimmune myocarditis (EAM) by decreasing the infiltration of inflammatory macrophages and inducing shift of macrophages in myocardium from both M0 and M1 to M2 phenotype. Based on

these observations and recent findings on microglia activation (Tocharus et al., 2012; Mercanti et al., 2014), curcumin and its analogues represent promising lead compounds targeting immune cells activation. The possibility to promote a macrophage protective phenotype has therefore become a therapeutic goal in the treatment of inflammatory conditions, and the identification of factors that control cell activation is currently an area of active research.

2. Aim

New data are redefining macrophages as diverse, polyfunctional and plastic cells that respond to the needs of the tissue at steady state and during disturbed homeostasis. Inflammation plays a critical role in the onset and progression of degenerative diseases, and is characterized by activation of tissue-resident macrophages as well as monocyte-derived macrophages that originate and renew from the adult bone marrow. Under normal conditions these cells provide immune surveillance and host defense in the tissues to maintain homeostasis. However, upon sensing changes in the microenvironment, macrophages become activated, undergoing a morphological and functional switch (Sica and Mantovani, 2012). Activation of these cells is not an "all-or-none" process, but rather a *continuum* characterized by a wide *spectrum* of molecular and functional phenotypes ranging from the "classical" M1 activated phenotype, with a highly pro-inflammatory profile, to the "alternative" M2 phenotype, associated with a beneficial, less inflammatory, protective profile (Toniolo et al., 2014). However, recent advances in macrophage development, activation and functional diversity shape the understanding of macrophage biology and drive new models of activation and classification, away from the classical dichotomous categorization as M1 and M2 macrophages and into more complex models that can accommodate the *continuum* of transcriptional and functional states observed *in vivo*. Various pathologies, ranging from obesity to autoimmunity and neurodegenerative disease, have been linked to the dysregulation of macrophage function.

The diversity of terminology and inconsistent use of markers to describe macrophage activation impedes reaching a *consensus* in this research field. In particular, a critical issue is the diversity in macrophage activation across species. Similarly, cell lines (i.e. THP-1) as opposed to primary cultures are widely used as macrophage models. CSF-1-cultured macrophages from murine bone marrow and human peripheral-blood monocytes remain the predominant *in vitro* systems used for generating macrophages. In general, the culture conditions for generating the two paradigmatic *in vitro* M1 and M2 populations are straightforward, i.e., post differentiation stimulation with IFN-γ or IL-4. Given the lack of gold standards for M1 or M2 activation, we previously demonstrated that (a) the cell population

resulting from spontaneous differentiation has predominance of the M2 over M1 phenotype as measured by flow cytometry, and (b) the expression of M1 vs. M2 markers is not mutually exclusive (Tedesco et al., 2015). However, patterns of macrophage activation may differ based on experimental protocols used by labs active in the field. Therefore, differentiation and activation protocols appear to be crucial, as shown e.g. by recent guidelines and comparison studies (Vogel et al., 2014; Murray et al., 2014).

This is especially relevant when testing the potential impact of pharmacological interventions targeting macrophage function. In fact, there is wide interest in the development of diagnostic and therapeutic approaches targeting polarized inflammation and macrophage activation phenotypes. For instance, by employing a variety of experimental designs, PPARγ agonists (Bouhlel et al., 2007) and statins (van der Meij et al., 2013) have been shown to promote M2-like polarization, whereas glucocorticoids induce an M2c activation state (Mantovani et al., 2004; Ambarus et al., 2012a). However, translation of this knowledge basis to clinical application may be hampered by the plurality of experimental protocols associated with the remarkable plasticity of cells of the mononuclear phagocyte lineage. Deployment of therapeutic macrophage modulators therefore requires that standards be translatable across disciplines so that pharmaceutical and regulatory bodies can draw meaningful comparisons in terms of diagnostic or efficacy metrics.

On these grounds, the **specific aims** of the present thesis were: a) to test cell models and differentiation protocols other than spontaneous blood-derived macrophage differentiation (Tedesco et al., 2015), namely the THP-1 cell line and CSF-1-driven differentiation, respectively; b) to profile the cytokine pattern into the culture medium, and c) to determine the modulation of phenotypic markers by pharmacological agents, namely curcumin derivatives known to suppress microglial activation through reduced production and release of pro-inflammatory mediators (Mercanti et al., 2014), as well as the underlying mechanisms of action.

3. Materials and Methods

3.1. MATERIALS

RPMI 1640 was purchased from LONZA (Basel, Switzerland), antibiotics solution (100 U/ml penicillin and 100 µg/mL streptomycin) from Invitrogen Inc. (Carlsbad, CA, US). Monoclonal antibodies anti-human COX-1 and COX-2 were from Cayman Chemical (Ann Arbor, MI, US), and anti-human IκB-α and GAPDH were from Cell Signaling (Danvers, MA, US). HRP-conjugated secondary antibodies were purchased from Vector (Peterborough, UK). anti-CCR2 mAb, anti-CD163 mAb, anti-IL-1β mAb, brefeldin, Fix and Perm buffer solutions were from eBioscience/Affymetrix (Santa Clara, CA, US); anti-CD80 mAb, anti-CD206 mAb from BD Biosciences Pharmigen (San Diego, CA, US). RevertAid Reverse Transcriptase, random examers, nucleotides, RNAse inhibitors and Max SYBR Green PCR Master Mix were purchased from Thermo Fisher (Waltham, MA, US). Complete protease inhibitor mixture was from Roche (Mannhein, Germany). Hematoxylin and eosin, fetal bovine serum (FBS), Ficoll-Paque (density 1.077±0.001), Percoll, dexamethasone, curcumin, CLI095, lipopolysaccharide (LPS), skim milk powder as well as other analytic grade chemical agents were purchased from Sigma-Aldrich (St. Louis, MO, USA). IFN-γ, IL-4, IL-13 and CSF-1 were from Immuno Tools GmbH (Friesoythe, Germany). Curcumin analogues were kindly provided by Dr. Federica Belluti (Department of Pharmacy and Biotechnology, University of Bologna, Italy).

Experimental protocol

The experimental protocol is outlined in Fig. 3.1:

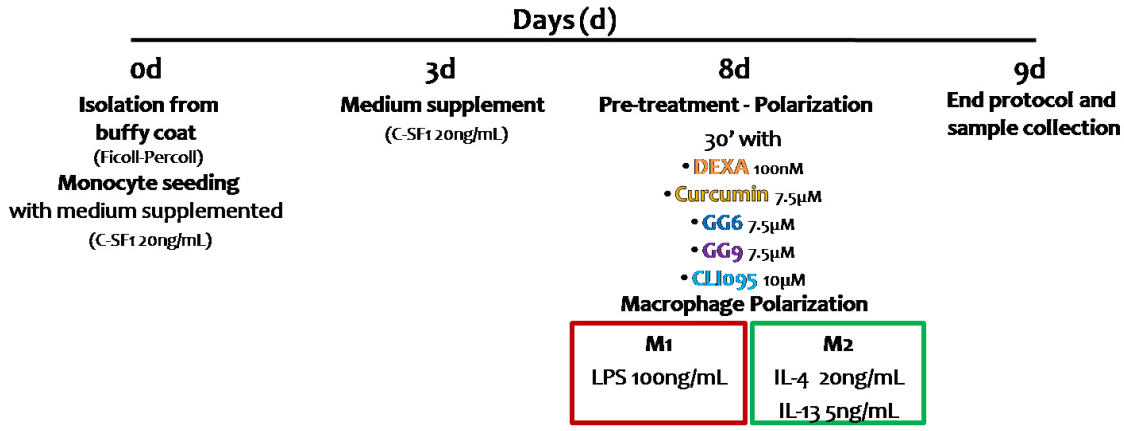

Figure 3.1. A schematic line drawing the experimental approach

3.2. CELL CULTURE

Human peripheral mononuclear cells (PBMCs) were isolated from buffy coats provided by the Transfusion Unit at Padua University Hospital. The buffy coat is the fraction of an anticoagulated sample that contains most of the white blood cells and platelets following density gradient centrifugation of the blood. Blood samples from 20 healthy donors were processed.

3.2.1 Ficoll gradient and spontaneous differentiation

PBMCs were isolated by density gradient centrifugation using a Ficoll-Paque solution, a hydrophilic polysaccharide commonly used in biology laboratories to separate blood to its components (density 1.077±0.001). Ficoll-Paque was placed at the bottom of a conical tube, and blood was then slowly layered above it in a 20:15ml ratio. After being centrifuged at 600g for 30 min, different layers were visible in the conical tube, from top to bottom: plasma and other constituents, a white layer of mono-nuclear cells called buffy coat (PBMC/MNC), Ficoll-Paque, and erythrocytes & granulocytes. PBMCs were harvested using a sterile Pasteur pipette and transferred to a new centrifuge tube. To reduce platelet contamination, cells were washed twice with PBS + 5mM EDTA at 300g for 15 min. Cells were seeded at the density of $15x10^6$ cells in 100-mm dishes and $6x10^6$ cells in 60-mm dishes in serum-free RPMI 1640 medium supplemented with 100 U/ml penicillin and 100 µg/mL streptomycin. After 2h, non-adherent cells were removed by repeated washing and the remaining adherent fraction was cultured over 7 days at 37°C and 5% CO_2 in the presence of 10% FBS. The medium was not replaced throughout the culture period and no further exogenous agent was added in order to allow spontaneous monocyte differentiation into resting macrophages (M0).

3.2.2 Percoll gradient and CSF-1 driven differentiation

After the Ficoll separation PBMCs could be separated with a Percoll density gradient, to obtain pure monocytes. The separation of monocytes from lymphocytes was performed with a high-density hyper-osmotic Percoll density gradient: the PBMC suspension, containing $150\text{-}200x10^6$ cells, was layered above it

in a 1:3.33ml ratio. After being centrifuged at 600g for 15 min, the cells at the interface were collected and washed with serum-free RPMI, counted and seeded in RPMI +10% FBS in the presence of 20 nM CSF-1 (Repnik et all, 2003). Cells were cultured over 7 days at 37°C and 5% CO_2, and the medium was changed every three days, adding fresh CSF-1.

Cell morphology was monitored during both differentiation transitions from monocyte to macrophages as well as at the end of polarization protocols, and images were recorded using a phase contrast Nikon Eclipse Ti-S microscope (20x or 40x magnification).

3.3. PROTOCOLS OF POLARIZED ACTIVATION

After removing the culture medium of differentiation, M0 macrophages were polarized toward M1 phenotype by incubation with LPS (0.1-1 μg/ml) for 24 or 48h. M2 polarization was obtained by adding IL-4 (20 ng/ml) and IL-13 (5 ng/ml) for 24 or 48h. In selected experiments M0 cells were challenged overnight with either 100 nM dexamethasone or 30-min pre-treatment with curcumin analogues before polarized activation (Table 3.1). As an internal positive control to confirm the possible effect of our curcumin-based analogues on the TLRs pathway we used CLI095 (Sigma). CLI-095, also known as TAK-242, is a novel cyclohexene derivative that suppresses specifically TLR4 signaling, inhibiting the production of NO and pro-inflammatory cytokines (Li et al., 2006). It acts by blocking the signaling mediated by the intracellular domain of TLR4, but not the extracellular domain. It potently suppresses both ligand-dependent and -independent signaling of TLR4 (Kawamoto et al., 2008).

After polarization, macrophages were harvested by gently scraping culture plates with 1ml PBS containing 5 mM EDTA and 2% FBS for qPCR and Western blot analysis. Additional cell samples were collected in a round bottom tube for flow cytometry for phenotype characterization and cytokine detection, and analyzed using a FacsCanto II flow cytometer (BD Biosciences Pharmigen San Diego, CA, US).

	Color of the solution	Concentration
Curcumin	yellow	7.5 µM
GG6	yellow	7.5 µM
GG9	No color	7.5 µM
CLI095	No color	1 µM

Table 3.1: Curcumin analogues concentration and characteristics.

To obtain *Macrophage Conditioned Media* (MCM) experiments were performed by polarizing the cells toward M1/M2 immunophenotypes for 48h as described above and incubating for further 72h in the absence of any activating agent. At the end of this period MCM was harvested and concentrated 10x using Amicon Ultra-15 centrifugal filter units with Ultracel-PL, cut-off 3 KDa (Millipore/Merk, Darmstadt, Germany). The MCM was stored at -20°C until further analysis using the Luminex Technology (Luminex Corporation, Austin, TX, US).

3.4. FLOW CYTOMETRY

3.4.1 Evaluation of leukocyte populations in a whole blood sample

We first analyzed the different leukocyte populations (lymphocytes, monocytes, granulocytes) in a sample of whole blood collected from the buffy coat used for monocyte separation. Blood was diluted 1:2 with saline buffer (0.9% NaCl) and then incubated with 2 ml of lysis buffer 1 (0.2% NaCl w/v) for 10 min at room temperature to lyse the erythrocytes, followed immediately by the addition of lysis buffer 1 (1.6% NaCl, 0.2% sucrose) for a further 10-min incubation. The sample was centrifuged at 300g for 5 min at room temperature, and the white cell pellet was washed twice in PBS/EDTA, suspended in 500 µl of PBS containing 2% FBS and analyzed by flow cytometry (Beckman Coulter Epics XL). A two-dimensional dot plot hystogram displayed a light scatter plot of white blood cells passing through a flow cytometer. The X-axis shows forward light scatter (FS) indicative of cell size,

whereas the y-axis shows side light scatter (SS) indicative of cell granularity. The correct voltage settings of these two parameters permitted to discriminate the free PBMCs populations.

3.4.2 Identification and characterization of monocyte subsets

Identification of monocyte subsets was performed using multiparameter flow cytometry. For analysis of classical and non-classical monocytes, cells were stained with a FITC or phycoerythrin (PE) anti-CD14 monoclonal antibody (mAb). The analysis was performed according to standardized gating strategy (Ziegler-Heitbrock et al., 2010). The relative frequency of these monocyte subsets were expressed as the percentage of the total monocyte gate.

3.4.3 Characterization of human macrophage phenotypes by flow cytometry

Human macrophages were harvested by gently scraping culture plates with PBS containing 5 mM EDTA, collected in round-bottom tubes for immunolabeling (BD Biosciences) and resuspended at 10^6/ml in 100 µl PBS with 2% FBS to block Fc receptors. Purity in these cultures was first assessed by staining cells with PE-anti-CD14 (20 µl/10^6 cells), which is a well-known circulating monocyte marker, also expressed on mature macrophage surface; furthermore, we excluded lymphocyte contamination by staining cells with PeCy7-labeled antibody against CD3 (5µl/10^6 cells), an antigen bound to the membranes of all mature T-cells.

In order to characterize the phenotypes of spontaneously human monocyte-derived macrophages, we analyzed specific surface marker expression of resting, M1 and M2 polarized immunophenotypes. Macrophages were stained for 30 min in the dark with fluorochrome-tagged monoclonal antibodies against surface CD80-FITC (20µl/10^6 cells) and CCR2-APC (10µl/10^5 cells) to typify the M1 phenotype, and against CD206-FITC (20µl/10^6 cells) and CD163-PE (20µl/10^6 cells) to characterize the M2 phenotype. The last panel of M1/M2 markers was selected based on a characterization performed in human monocytes (Fadini et al, 2013). After incubation with specific antibodies, samples were washed and suspended in 250 µl PBS/EDTA, and 10,000 events/sample for each tube were recorded in a FacsCanto II

flow cytometer (BD Biosciences). Data were analyzed using the FacsDiva software (BD Biosciences). Isotype-matched controls were used as a reference.

Expression of each surface antigen and its modulation after stimulus was evaluated individually or in combination with other markers, in order to explore how polarization can affect macrophage phenotypes by down-regulating or enhancing surface protein expression or localization within the cells. During analysis, typically less than 2% positive cells were allowed beyond the statistical marker in appropriate controls.

3.4.4 Intracellular cytokine production

Intracellular cytokine production was evaluated using flow cytometry in monocyte-derived macrophages. After spontaneous differentiation, macrophages were stimulated with either LPS (1 μg/ml) or IL-4 (20 ng/ml) plus IL-13 (5 ng/ml) for 6 h. Cells were pretreated with brefeldin (10 μM) to block cytokine secretion. At the end of stimulus, cells were harvested by gently scraping culture plates with 1 ml PBS containing 5 mM EDTA and 2% FBS. Cells were collected in a round bottom tube for flow cytometry and processed for immunostaining.

Where indicated, whole blood samples or monocyte-derived macrophages were treated with 100 nM dexamethasone overnight or with curcumin analogues 30 min before stimulation.

Macrophage pellets were fixed with 100 μl 4% paraformaldehyde solution and permeabilized by adding 2 ml of Perm Buffer solution containing 0.1% saponin and 0.009% sodium azide. Cells were centrifuged twice and incubated in 100 μl Perm Buffer solution in the presence of FITC-anti-IL-1β (5 μl/10^6 cells) for 20 min in the dark. Subsequently, cells were washed, resuspended in 250 μl PBS/EDTA, and 10,000-50,000 events/sample for each tube were recorded.

3.5. GENE EXPRESSION ANALYSIS

Total RNA was isolated from about $6x10^5$ cells. Cells were washed once in PBS and RNA was extracted using the RNeasy Plus Mini Kit (Qiagen, Switzerland). cDNA was generated from 200 ng total RNA (nanodrop Thermo Scientific, Reinach, Switzerland) using RevertAid Reverse Transcriptase and random primers according to the manufacturer's instructions. The relative quantification of the genes of interest was measured by real-time quantitative PCR (Q-PCR) performed using Max SYBR Green PCR Master Mix for 40 cycles of denaturation (15 sec, 95°C), annealing (30 sec, 60°C) and extension (30 sec, 72°C) on a CFX96 Real-Time PCR Detection System thermocycler (Biorad, Milan, Italy). Oligonucleotide primers were designed using the online tool for Real-Time PCR Blast and obtained from Invitrogen. The primer sequences are shown in Table 3.2. Results were normalized using the housekeeping gene 18S, GAPDH and the ΔΔ cycle threshold method, and are expressed as relative fold of stimulated over control group, used as calibrator.

	Forward	Reverse
18S	AAACGGCTACCACATCCAAG	CCTCCAATGGATCCTCGTTA
GAPDH	CACCATCTTCCAGGAGCGAG	CCTTCTCCATGGTGGTGAAGAC
TNF-α	TCCTTCAGACACCCTCAACC	AGGCCCCAGTTTGAATTCTT
IL-1β	GGGCCTCAAGGAAAAGAATC	TTCTGCTTGAGAGGTGCTGA
IL-10	TGCAAAACCAAACCACAAGA	TCTCGGAGATCTCGAAGCAT

Table 3.2: qPCR primer sequences for the phenotypic characterization. The primers were designed using the online tool for Real-Time PCR Blast.

3.6. WESTERN BLOT

For protein extraction, $6x10^5$ cells were seeded in 60-mm dishes. After polarized activation, cells were washed once with PBS and harvested in 150µl lysis buffer (50 mM Tris HCl pH 7.4, 150 mM NaCl, 1% NP-40, 25mM NaF, 0.5% Na desoxycholate, 10% SDS, 1mM EGTA, 1 mM sodium orthovanadate, 10 mM sodium pyrophosphate, 1 mM phenyl-methyl-sulfonyl-fluoride (PMSF) and Complete® protease inhibitors (Roche). Each sample comprised two pooled plates and was stored at -20°C until further analysis. Protein concentration was determined by protein assay using Lowry protocol and reagents (Lowry et al., 1951). Protein lysates were heated at 100°C for 5 min to denature proteins and 40 µg of each sample were loaded onto a 10% SDS/polyacrylamide gel and run at 120V for 1h. Cell proteins were then transferred to PVDF membrane at 100V for 1h at room temperature, using a 25mM Tris, 192nM glycine and 20% methanol buffer. The membrane was blocked with 5% milk in TBS (1M Tris HCl pH 7.4, 5M NaCl, 0.1% Tween 20) for 1h at room temperature, washed, and then incubated with specific primary antibodies against IκB-α and GADPH (Table 3.3). Immunolabeled proteins were detected by using appropriate HRP-conjugated secondary antibodies, and immunoreactive bands were revealed using enhanced chemiluminescence (ECL) detection. Band intensities were normalized to GADPH. The intensity of each blot was measured using the ImageJ software.

Protein primary antibody			Secondary antibody	
	Origin	Dilution		Dilution
IκB-α	Rabbit monoclonal	1:1000	Anti- rabbit	1:5000
GAPDH	Rabbit monoclonal	1:1000	Anti- rabbit	1:5000

Table 3.3: Antibodies used for Western blot analysis

3.7. ELISA ASSAY

Monocytes were plated in 24-well plates at a density of 10^6 cells per well, respectively, using culture medium and allowed to differentiate for 7 days. Cells were primed by pre-treating with 1 μg/ml LPS or other TLR ligands as indicated in the presence or absence of curcumin analogues (optimal concentration of TLR activator chosen from preliminary experiments) for 6 h in culture medium (Ferrari et al, 1997). The TLR ligands used did not affect cell viability. It should be pointed out that commercial sources of LPS are frequently contaminated by other bacterial components, such as lipoproteins, capable of activating both TLR2 and TLR4. The Ultra-Pure LPS-EB preparation used here only activates TLR4 (InvivoGen). Cell supernatants were collected and stored at −20°C until the day of assay (avoiding repeated freeze-thaw cycles). Cell lysates were prepared by adding to each 24-well culture 40 μl of lysis solution. The IL-1β content of culture medium and cell lysates was analyzed using commercially available enzyme-linked immunosorbent assay (ELISA) kits according to the manufacturer's instructions (Antigenix America, Huntington Station, NY, USA). The IL-1β ELISA assay kit does not distinguish between the inactive 31-kDa precursor (pro-IL-1β) and the bioactive 17-kDa mature form (as is the case for all commercially available kits). Standards with known amounts of IL-1β were used to convert values into absolute concentrations of IL-1β in pg/ml.

3.8. STATISTICAL ANALYSIS

Statistical analysis was performed using Prism software (GraphPad Software Inc, La Jolla, CA, US). Data were expressed as mean ± SEM. ANOVA followed by Bonferroni *post-hoc* test were used for comparison between samples. A P value < 0.05 was considered to be statistically significant.

4. Results

4.1. HUMAN MONOCYTE-DERIVED MACROPHAGE CULTURES

4.1.1 Leukocyte distribution in human peripheral blood samples

We initially evaluated leukocyte populations in human blood samples by flow cytometry. Fig. 4.1 shows a two-dimensional dot plot histogram displaying a light scatter plot of white blood cells obtained from buffy coats after erythrocyte lysis passing through a flow cytometer. In particular, the x-axis shows forward light scatter (FS) indicative of cell size, whereas the y-axis shows side light scatter (SS), indicative of cell granularity. The correct voltage settings of these two parameters allow large and very granular cells (granulocytes) to be differentiated from the smaller, less granular cells (monocytes) and, furthermore, from the even smaller lymphocytes. In particular, in the representative plot shown below, monocytes represented about 10% of total leukocytes in human blood, as reported previously (Auffray et al., 2009).

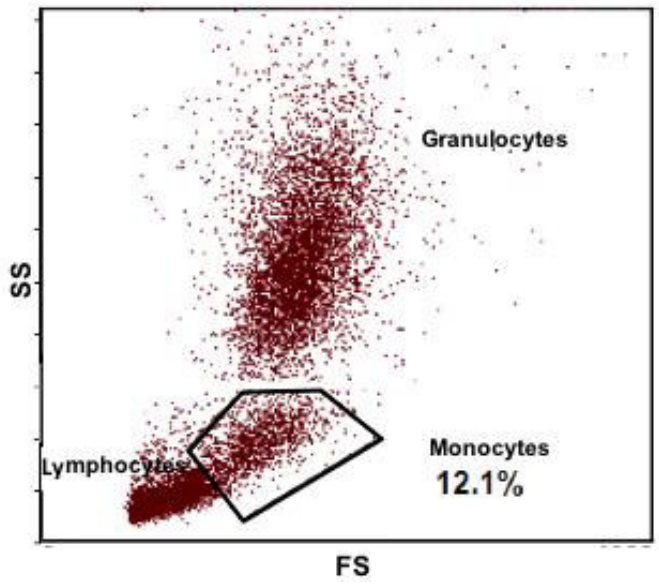

Figure 4.1: The three main components of human leukocytes (lymphocytes, monocytes and granulocytes) are represented on the dot plot following flow cytometry. The three distinct populations can be distinguished based on their size and cell complexity (granularity).

4.1.2 Characterization of human monocyte-derived macrophages

Blood samples from buffy coats were stratified on a Ficoll-Paque solution and the lympho-monocyte fraction was separated by density gradient centrifugation. The PBMC ring was then stratified upon a hyperosmotic Percoll solution to obtain pure monocytes that were cultured in the presence of CSF-1 (Fig. 4.2, right panels). After plating, morphology and size of adherent monocytes were observed over the differentiation period. Cell growth and differentiation were monitored from day 1 to 6. We observed that at day 1 monocytes were small and round. As expected, at day 3 of culture they showed a larger cytoplasm volume than that of monocytes, possibly due to increased cytosolic organelle size (Fig. 4.2), which further increased till day 6. A largely comparable differentiation profile characterized FBS-driven macrophages culture (Tedesco et al., 2015).

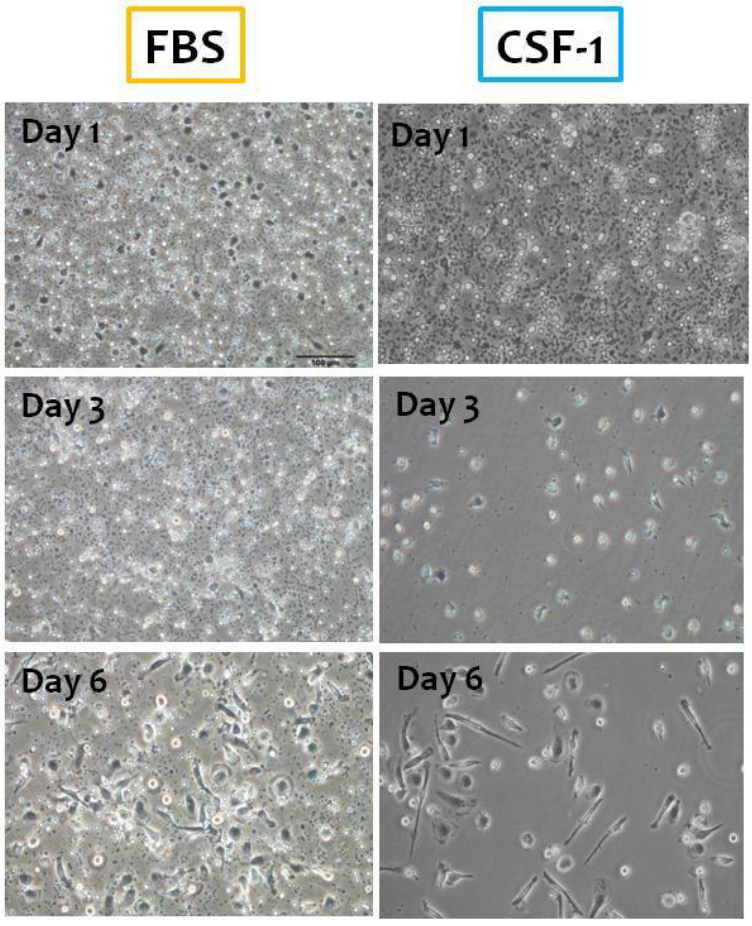

Figure 4.2: Morphological changes of monocytes during differentiation into macrophages. 20x magnifications, Nikon Eclipse Ti microscope.

In order to determine the extent of lymphocyte contamination, both cultures were stained with antibodies against CD14 (for monocytes-macrophages) and CD3 (for lymphocytes) surface markers. In FBS-driven macrophages at day 1, about 30% of adherent cells were found to be $CD3^+$, while during the differentiation period the lymphocyte fraction declined progressively until day 8, when only about 15% of cells were $CD3^+$. In contrast, in the CSF-1-driven macrophage population at day 1 about 3% of adherent cells were $CD3^+$ but this percentage fell to 0% at day 8. A representative experiment in Fig. 4.3 for FBS-driven macrophages at the end of the differentiation period showed 76.4% of $CD14^+$cells (blue events) and 17.4% of $CD3^+$ cells (green events), respectively, while CSF-1-driven macrophages showed 89.2% of $CD14^+$cells (blue events) and 0% of $CD3^+$ cells (green events), respectively. Thus, at the end of the differentiation period, a minor fraction of $CD3^+$ cells was detectable in our FBS-macrophage culture consistent with previous studies using a similar differentiation protocol (Eligini et al., 2013), but a pure culture (0% $CD3^+$) was obtained using the CSF-1 protocol.

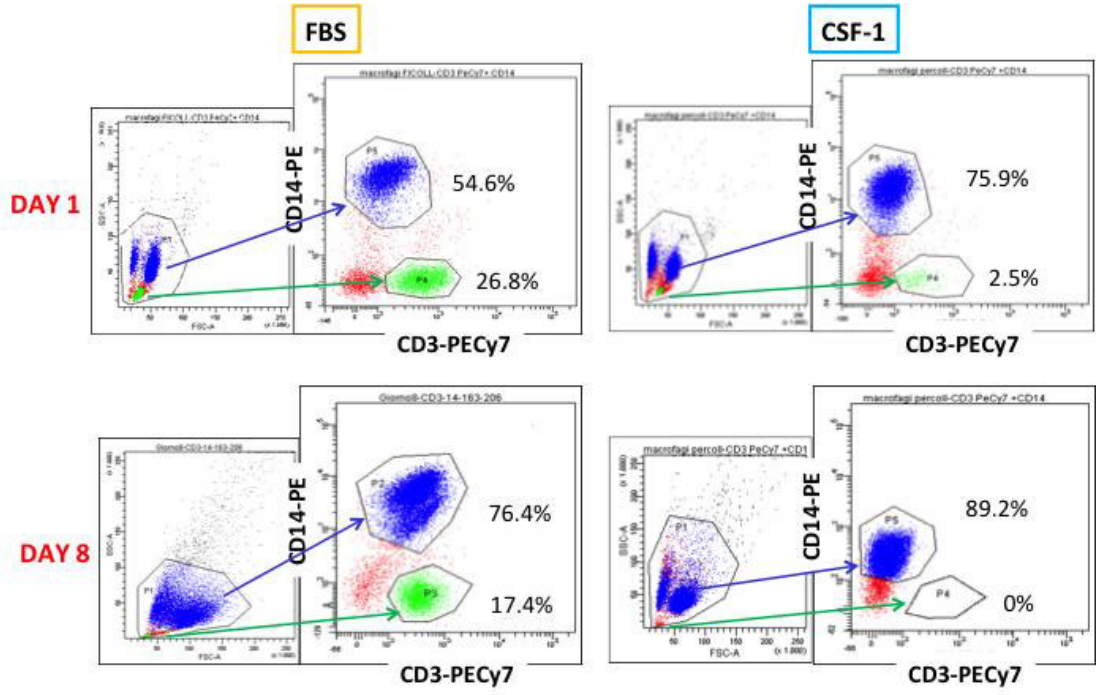

Figure 4.3: Representative flow cytometry dot plots of surface CD3 and CD14 expression in a 7-day culture of monocyte-derived macrophages. Cells were stained with PeCy7-anti CD3 antibody for the lymphocyte population (green events) and PE-anti CD14 antibody for the macrophage population (blue events). The back-gating strategy allowed localizing these populations within the FS/SS plot (lower left panel).

We then characterized the resting macrophage phenotypes by flow cytometry at day 8 of differentiation (Fig. 4.4). A fraction of the cells from both protocols stained positively for the surface M1 markers CD80 and CCR2 and for the M2 markers CD206 and CD163. FBS- (Fig. 4.4A) and CSF-1-driven (Fig. 4.4B) resting macrophages displayed a predominant M2 vs. M1 phenotype, as defined by positive staining for CD163 and CD206. In both protocols these percentages reflected "mixed activated" cells expressing varying levels of the different M1 or M2 markers, but with a major subpopulation that was more M2-oriented than M1-oriented.

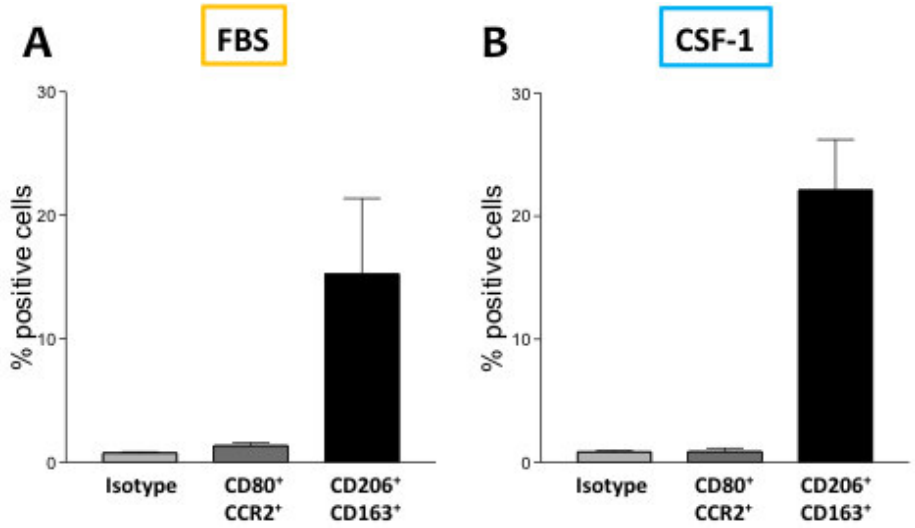

Figure 4.4: Phenotypic markers of resting human monocyte-derived macrophages at day 8 of differentiation. Bar graph of FBS- (panel A) and CSF-1- (panel B) driven macrophages show the percentage of M1 ($CD80^+/CCR2^+$) and M2 cells ($CD206^+/CD163^+$)as mean (± SEM) of 4 independent experiments.

4.2. IMMUNOPHENOTYPING OF CSF-1 DIFFERENTIATED MACROPHAGES

Immunophenotypes of CSF-1-driven human monocyte-derived macrophage were further characterized by analyzing specific surface markers expression in cells cultured in the growth medium supplemented with CSF-1 (M0) or in the presence of a pro- (LPS) or anti-inflammatory (IL-4/IL-13) microenvironment.

4.2.1 Characterization of macrophage morphotypes

At the end of differentiation, resting macrophages (M0) showed two dominant and distinct morphotypes as observed by phase contrast microscopy (Fig. 4.5): spindle/elongated and round-"fried-egg" shaped, which routinely occurred in resting cultures consistent with recent studies (Eligini et al., 2013; Ambarus et al., 2012a). Following 24h activation with either LPS to induce the M1 phenotype or with IL-4/IL-13 to obtain the M2 phenotype, cell morphology changed: in fact, M1-polarized macrophages were enriched in the long and spindle-shaped morphotype (Fig. 4.5B), while M2 polarized macrophages were largely round-shaped (Fig. 4.5C). These observations suggest that polarized activation affected macrophage morphology.

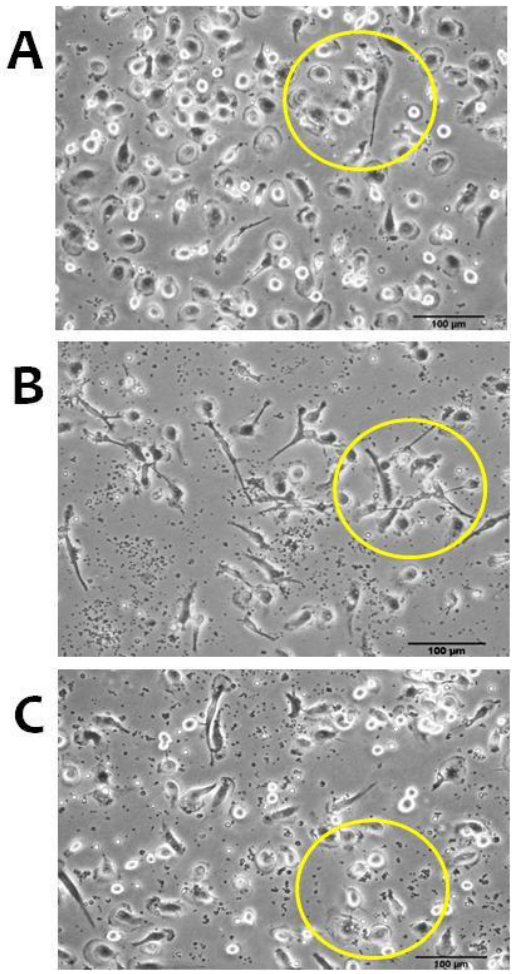

Figure 4.5: Phase contrast images of macrophages differentiated from monocytes, in resting state (M0, A) and after activation with LPS (M1, B) or IL-4/IL-13 (M2, C) for 24h. Circles indicate the CSF-1-differentiated macrophage heterogeneous population (A) and enrichment for the two main spindle-shaped (B) or round (C) morphotypes. Representative images were captured from macrophages obtained from the same donor. 20x magnification, Nikon Eclipse Ti microscope.

4.2.2 Characterization of the M1 macrophage subset

We then analyzed the fraction of M1 macrophages by flow cytometry as defined by either positive single-staining for CD80 and CCR2 or by specific double-staining of $CD80^+/CCR2^+$ cells. Graphs in Fig. 4.6 show that, under resting conditions, 7.7±5.0% of M0 macrophages were $CD80^+$(panel B) and 1.1±0.57% were $CD80^+/CCR2^+$ (panel D; see also the representative flow cytometry analysis in Fig. 4.6A). Following incubation with LPS for 24h, the amount of $CD80^+$ macrophages increased (35.8±8.6 *vs.* 7.7±5.0%, p<0.02; n=4, Fig. 4.6B; see also Fig. 4.6A) and a tendency was observed for $CCR2^+$ cells as well (24.3±12.9 *vs.* 4.8±1.7%; n=4, Fig 4.6C). A significant modulation of $CD80^+/CCR2^+$ cells was observed, compared with resting macrophages (4.6±1.07 *vs*. 1.1±0.57%; p<0.02; n=4, Fig. 4.6D; see also Fig. 4.6A red box). M2 polarized activation with IL-4/IL-13 did not significantly affect the fraction of $CD80^+$ and $CD80^+/CCR2^+$ cells compared with resting macrophages (4.2±1.3 *vs.* 7.7±5.0% for $CD80^+$ cells and 1.1±0.3 *vs* 1.1±0.6% for $CD80^+/CCR2^+$ cells, respectively; panel B and D, n=4).

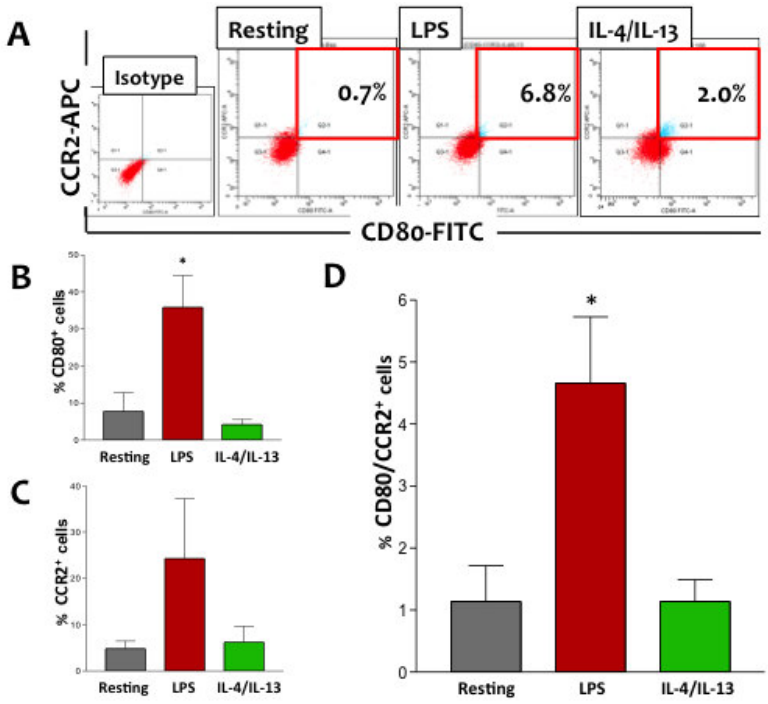

Figure 4.6: Staining of M1 macrophages as defined by $CD80^+$ and $CCR2^+$ cells. Cells were differentiated from monocytes in RPMI 1640 + 10% FBS + CSF-1 for 7 days and thereafter activated with LPS or IL-4/IL-13 for 24h. Fluorescence quantification dot plots (A) are from a representative experiment: red boxes highlight $CD80^+/CCR2^+$cells and their modulation after M1 and M2 polarization. Bars represent the mean (±SEM) of $CD80^+$ (panel B), $CCR2^+$ (panel C) and $CD80^+/CCR2^+$ (panel D) cells from 4 independent experiments. *p<0.02 *vs* resting.

4.2.3 Characterization of the M2/anti-inflammatory macrophage subset

We next analyzed the M2/anti-inflammatory subset by flow cytometry as defined by $CD163^+$, $CD206^+$ or specific double $CD206^+/CD163^+$ staining. In resting state, 63.1±3.7% of cultured macrophages were $CD206^+$, and 5.8±1.7% were $CD163^+$. After polarization with LPS, the percentages of $CD206^+$ as well as $CD163^+$ cells significantly decreased compared with resting macrophages (43.1±4.1 *vs* 63.1±3.7% $CD206^+$, Fig. 4.7B; 1.6±0.8 *vs.* 5.8±1.7% $CD163^+$, $p<0.05$, n=3, Fig. 4.7C). Similarly, LPS treatment decreased the abundance of the double-stained $CD206^+/CD163^+$ cell subpopulation with respect to resting macrophages (0.9±0.4 *vs* 5±1.3% $CD206^+/CD163^+$, $p<0.05$, n=3, Fig. 4.7D; see also Fig. 4.7A, green box). Following activation with IL-4/IL-13 for 24h, the percentage of cells specifically stained for each marker did not differ from that in resting cells (Fig. 4.7B and C). Similar results were obtained for the $CD206^+/CD163^+$ subpopulation (Fig. 4.7D).

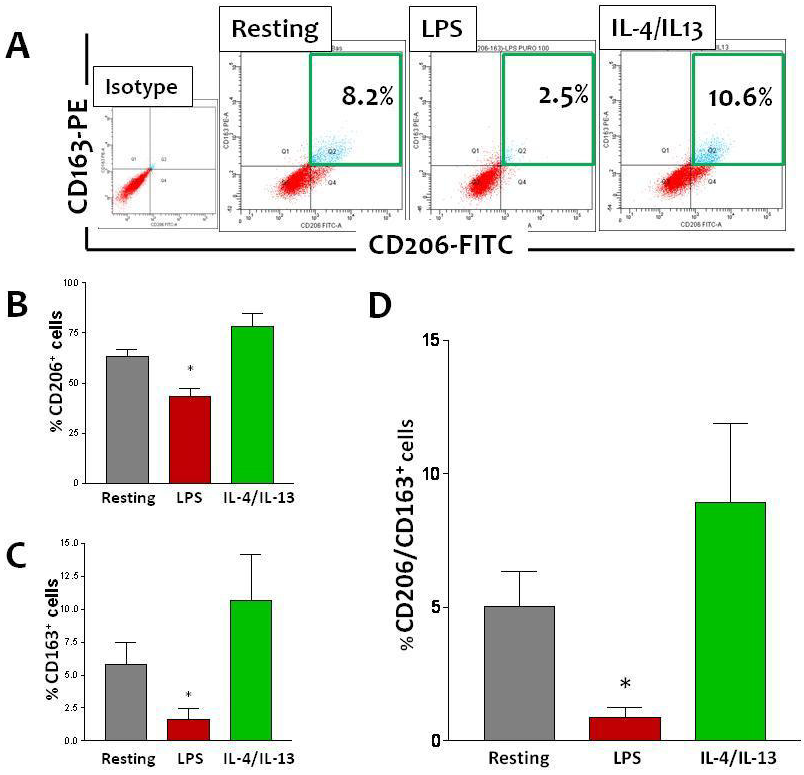

Figure 4.7: Quantification of M2 macrophage markers as percentage of $CD206^+$, $CD163^+$cells. CSF-1 differentiated macrophages were polarized as described in the legend to Fig. 4.6 above and stained with FITC-anti-CD206 and PE-anti-CD163 specific antibodies. Fluorescence quantification dot plots (A) are from a representative experiment: green boxes highlight $CD206^+/CD163^+$ cells. Bars represent the mean (±SEM) of $CD206^+$ (panel B), $CD163^+$ (panel C) and $CD206^+/CD163^+$ (panel D) cells of 3 independent experiments. *$p<0.05$ *vs* resting.

We then performed a set of experiments with the human monocyte cells line THP-1 to further validate our methods and markers in a condition of total absence of $CD3^+$ cells. THP-1 derives from human acute monocytic leukemia and can be differentiated to macrophages by adding phorbol ester (TPA, 185nM) for 6h *in vitro* (Tjiu et al., 2009). We monitored the differentiation and activation (100 ng/ml LPS and 20 ng/ml IFNγ for M1; IL-4 20 ng/ml and IL-13 20ng/ml for M2 phenotypes, respectively) through contrast-phase microscopy (Fig. 4.8 panels A-C) and flow cytometry (Fig. 4.8 panels D-F). Like CSF-derived macrophages, THP-1 shown two main distinct morphotypes of elongated and round cells, routinely occurring in resting cultures (Fig. 4.8A). Morphology was further affected by subsequent polarization in that LPS/IFNγ-activated macrophages were enriched in the long and spindle-shaped morphotype (Fig. 4.8B), while IL-4/IL-13 activated THP-1 macrophages were largely round-shaped (Fig. 4.8C).

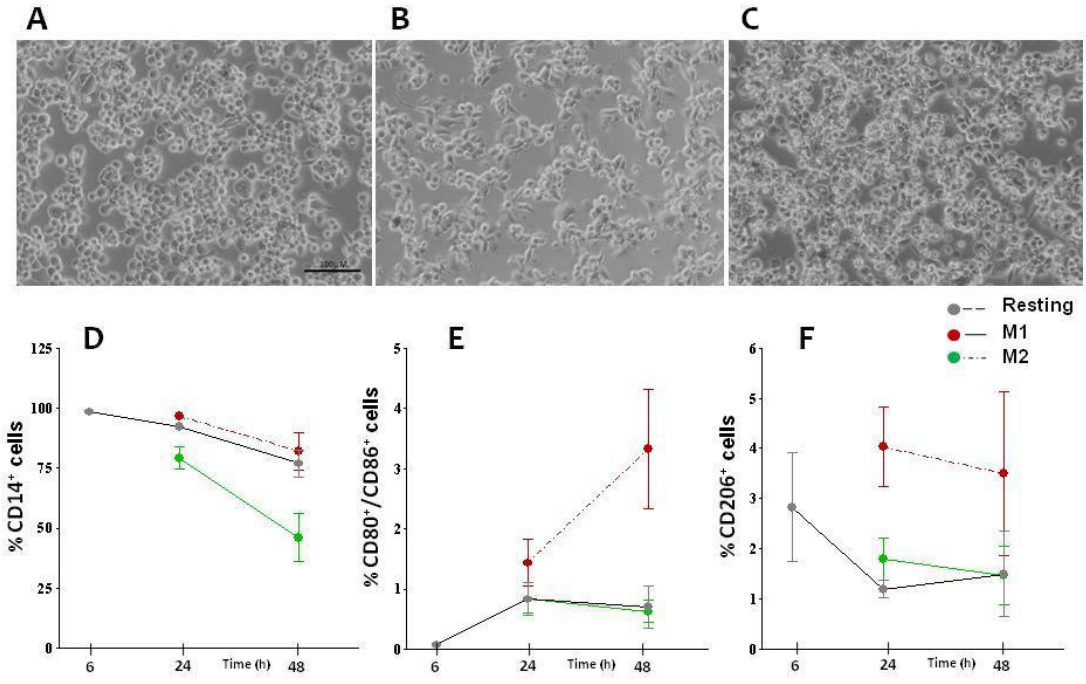

Figure 4.8: Contrast images of THP-1-derived macrophages. THP-1 monocytes were differentiated *in vitro* to macrophages in RPMI 1640 + 10% FBS in the presence of 185nM TPA for 6h. At this time monocytes were considered to be differentiated into resting macrophages (A), and thereafter activated with LPS/ IFNγ(B) or IL-4/IL-13(C) for 24 h. The cell population comprised two main round and spindle-shaped morphotypes. Representative images are shown, 20× magnification. THP-1 activated macrophages were stained with FITC-anti-CD14, PE-anti-CD86, PECy5-anti-CD80, APC-anti-CD206 and PECy5.5-anti-CD163 specific antibodies. Graphs represent the mean (±SEM) of $CD14^+$ (panel D), $CD80^+/CD86^+$ (panel E) and $CD206^+$ (panel F) cells of 3 independent experiments.

We then performed a time course by flow cytometry investigating the changes in CD14, CD80/CD86 (M1) and CD206/CD163 (M2) expression (Fig. 4.8 panels D-F). Fig. 8D shows that the percentage of $CD14^+$ cells was high (around 96%) after 6 h TPA and remained high also after 24h of M1- (red dots) or M2- (green dots) activation. Only after 48-h activation the level started to decrease in all samples (resting: from 92.1±0.6 at 24h to 76.8±5.7% at 48h; M1: from 96.5±0.3 at 24h to 82.1±7.8% at 48h; M2: from 79.1±4.6 at 24h to 46.1±10% at 48h). The double positive $CD80^+/CD86^+$ subpopulation used to describe the M1 phenotype increased after 24h, but more after 48-h LPS/IFNγ-activation (Fig. 4.8E). The $CD80^+/CD86^+$ cells were not affected in resting and M2 THP-1 cells, and remained low. THP-1 macrophages did not express detectable CD163 levels. The fraction of $CD206^+$ cells was low and did not increase after IL-4/IL-13 activation (Fig.4. 8F).

4.2.4 Analysis of macrophage conditioned medium

The composition of macrophage conditioned medium (MCM) was characterized by Luminex x-MAP technology plates used for all multiplex cytokine kits. A total of 50 predetermined analytes were analyzed and assays were run in triplicate according to the manufacturers' protocol. The fold-change for each individual cytokine for each of the multiplex kits is summarized in Fig. 4.9. As expected, M1 MCM showed the presence of high levels of pro-inflammatory cytokines and molecules like TNF-α, IL-1β, IL-6 and VEGF compared to resting MCM, while M2 MCM displayed high levels of IL-4 and CCL22 cytokines (bar graphs in the left part of Fig. 4.9, n=3). The anti-inflammatory cytokine IL-10 was unexpectedly more abundant in M1 than in M2 MCM, with a 3-fold increase *vs.* resting MCM; in M2 and resting MCM, the level of IL-10 were comparable. The right panel in Fig. 4.9 depicts all cytokines detected and their fold-change compared to resting MCM (all n=3).

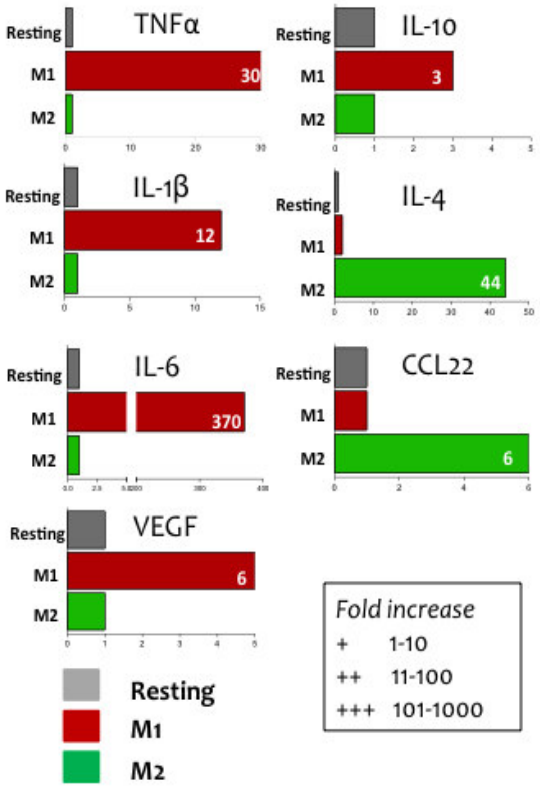

	Resting	M1	M2	Fold change	
IL-1α	1	65	1	++	
IL-2	1	2	2	+	+
IL-3	1	3	2	+	+
IL-5	1	1	1		
IL-7	1	2	1	+	
IL-8	1	89	0.2	++	-
IL-9	1	2	1	+	
IL-15	1	5	1	+	
IL-17	1	2	1	+	
IP-10	1	128	52	+++	++
MCP-1	1	3	0.4	+	-
MCP-3	1	5	0.4	+	-
MIP1α	1	14	1	++	
EGF	1	2	1	+	
FGF	1	19	1	++	
VEGF	1	6	1	+	
TGFα	1	6	3	+	+
G-CSF	1	16	2	++	+
GM-CSF	1	6	1	+	
IFNα	1	5	1	+	
IFNγ	1	70	2	++	+
PDGF-AA	1	1	1		
PDGF-BB	1	3	2	+	+

Figure 4.9: MCM composition of activated CSF-1 derived macrophages. Cells were polarized for 48h as described in the legend of Fig. 6 above and after activation FBS-free RPMI was added for 72h. Then the medium was collected, concentrated 10x and analyzed by Luminex x-MAP technology. 50 analytes were evaluated including cytokines, growth factors, cell adhesion molecules, immunoglobulin and components of immune system. The graphs and table summarize the fold-change for each individual cytokine of the multiplex kits. Data are shown as mean of 3 independent experiments run in triplicate.

4.2.5 Gene expression profile of target cytokines

We further characterized the immunophenotypes obtained after either M1 or M2 polarization by performing qRT-PCR analysis for TNF-α, IL-1β and IL-10 mRNA levels. In another set of experiments (see section 4.2.4 above) we analyzed the same cytokines released in the media by Luminex technology. After 6 h stimulation with LPS, macrophages showed higher mRNA levels of the genes encoding for TNF-α (3195±598 fold change, $p<0.05$, Fig. 4.10B) and IL-1β (516±64 fold change, $p<0.05$, Fig. 4.10A) compared with resting. The relative increase in mRNA levels after 48 h was more marked for IL-1β (4052±879 fold change, $p<0.005$) than that for TNF-α

(399±167 fold change, p<0.05). Conversely, mRNA levels for TNF-α rose more sharply after 6h and decreased after 48h (3195±598 fold change at 6h *vs.* 399±167 fold change at 48h, Fig. 4.10B). Macrophages stimulated for 6 and 48h with IL-4/IL-13 to enhance the M2 phenotype displayed comparable mRNA levels of genes encoding both IL-1β and TNF-α with respect to those of resting macrophages (Fig. 4.10, panels A and B respectively). The mRNA encoding the anti-inflammatory cytokine IL-10 was unexpectedly more abundant in LPS-treated (M1) cells than in those treated with IL-4/IL-13 (M2) at both time points (792±10 (M1) *vs* 2.5±0.6 (M2) fold change at 6 h, p<0.005; 11.3±3.5 (M1) *vs.* 3.6±2.5 (M2) fold change at 48 h; p<0.05, Fig. 4.10C). In particular, IL-10 mRNA peaked after 6h incubation with LPS (Fig. 4.10C).

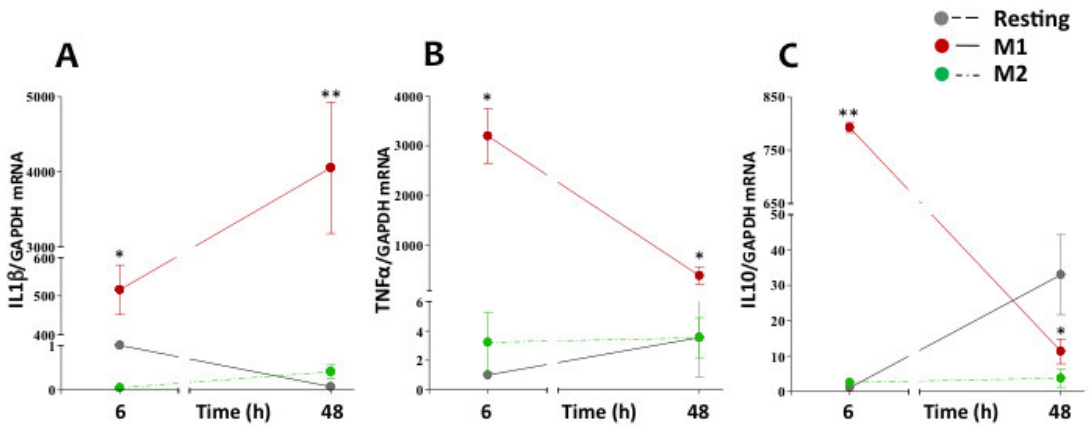

Figure 4.10: mRNA expression profiles of M1 and M2 phenotypic markers. Macrophages were differentiated from monocytes for 7 days in RPMI1640 + 10% FBS +CSF-1 and thereafter incubated with fresh medium (Resting, gray lines) or activated with LPS (M1, red lines) or IL-4/IL-13 (M2, green lines) for 6 or 48h. IL-1β (panel A), TNF-α (panel B) and IL-10 (panel C) mRNA levels were measured by Q-PCR and normalized to GAPDH. The mRNA level of selected genes in resting macrophages was assigned a value of 1, and mRNA levels following activation were shown relative to resting. Data are shown as mean (±SEM) of 3 independent experiments. *p<0.05 and **p<0.005 *vs.* resting.

4.3. PHENOTYPIC MODULATION BY CURCUMIN ANALOGUES

4.3.1 Specific staining of curcumin and curcumin analogues

To investigate the effect of curcumin on macrophage activation we performed flow cytometry experiments with curcumin and its analogues. One unexpected finding was that curcumin and GG6, but not GG9, interfered with the flow cytometer laser detection, showing high levels of positive cells for all fluorophores on the green laser (532-562 nM) as shown in the representative plots of Fig. 4.11 (after 24-h treatment: 4.6% $CD80^+$ cells in resting, 66.0% curcumin, 5.5% GG9 and 63.1% LPS groups, respectively). Because curcumin and GG6 yield yellow solutions, this pigment is able to interfere with the flow analysis. Based on these findings we decided to exclude these two compounds from further flow cytometry analysis.

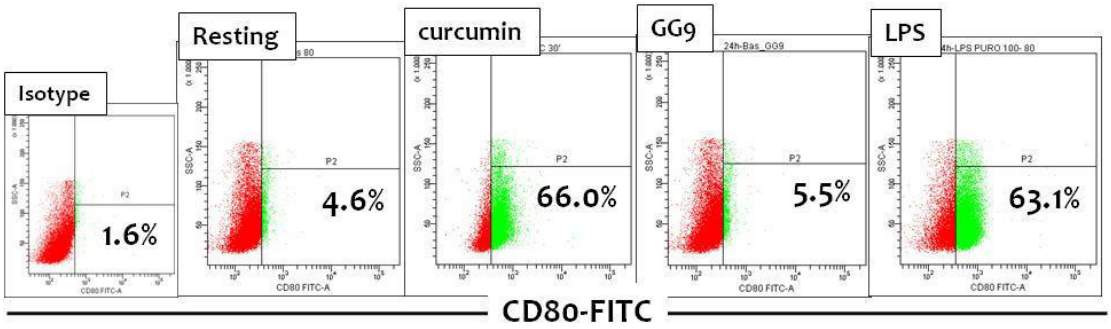

Figure 4.11: Percentage of $CD80^+$ cells after macrophage differentiation. The percentages described $CD80^+$ cells after 24h of stimulation with curcumin (7.5µM), GG9 (7.5µM) or LPS (100ng/mL). Fluorescence quantification dot plots from a single experiment.

4.3.2 Effects of dexamethasone and curcumin analogues on macrophage activation

We then evaluated the effect of dexamethasone (Dexa) and curcumin analogues on macrophage immunophenotypes after activation. Cells were pre-treated with dexa (100 nM), CLI095 (1 µM) or curcumin analogues (7.5 µM) for 30 min, and subsequently incubated with fresh medium to obtain resting macrophages (M0) or in the presence of either LPS or IL-4/IL-13 to obtain macrophages activated to M1 and M2 phenotypes, respectively.

First we investigated the effects of these compounds on M1 markers, expressed as $CD80^+$, $CCR2^+$ and $CD80^+/CCR2^+$ cells. As shown in Fig. 4.12B, the curcumin analogue GG9, as well as dexamethasone and CLI095, were able to significantly decreased the LPS-induced up-regulation of $CD80^+$ cells (LPS 42±6.2% *vs.* resting 10.1±3.5%, $p<0.005$, n=6, Fig. 4.12B) after 24h (dexa 11.2±3.6% *vs.* 42±6.2%, GG9 22.9±4.8 *vs.* 42±6.2%, CLI095 13.5±4 *vs.* 42±6.2%, $p< 0.05$, n= 6; Fig. 4.12B; see also Fig. 4.12A). No significant effects of curcumin analogues were seen in $CCR2^+$cells (Fig. 4.12C).

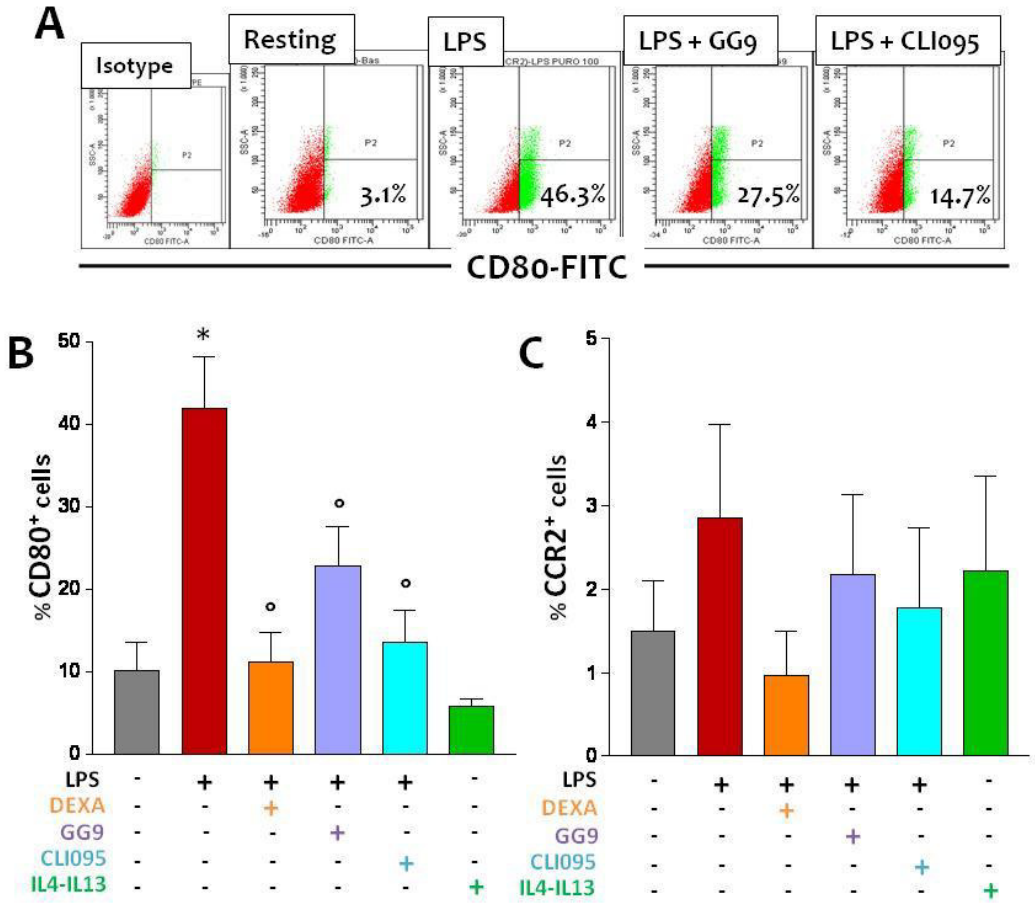

Figure 4.12: Fraction of M1 macrophages as defined by $CD80^+$and $CCR2^+$ cells. Cells were pre-treated with dexa and curcumin analogues for 30 min and then polarized as described in the legend to Fig. 4.6 above. Fluorescence quantification dot plots (A) are from a representative experiment. Bars represent the mean (±SEM) of $CD80^+$ (panel B) and $CCR2^+$ (panel C) cells from 6 independent experiments. *$p<0.01$ *vs* resting, °$p<0.05$ *vs* LPS.

No significant effects of curcumin analogues were observed on the double positive $CD80^+/CCR2^+$ cells (Fig. 4.13). Only pre-treatment with dexa was able to significantly prevent the up-regulation of $CD80^+/CCR2^+$ cells induced by LPS (0.7±0.3% *vs* 3±1.2%, °p<0.05, n=6, Fig.4.13).

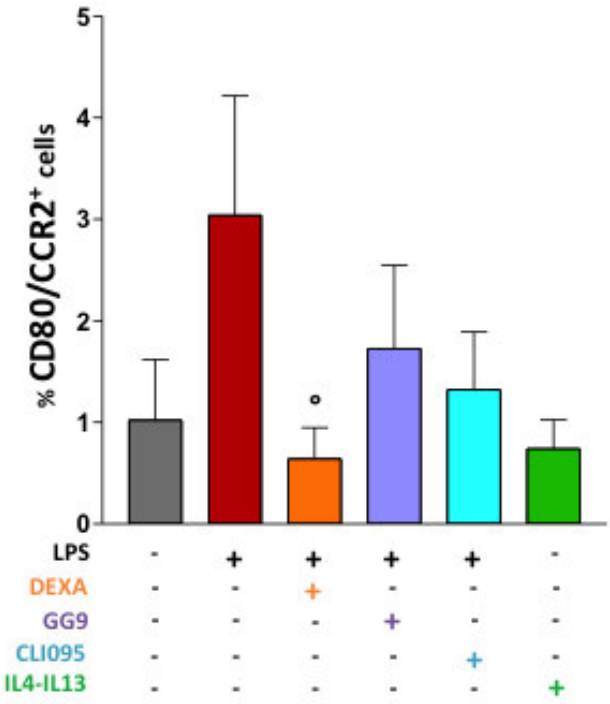

Figure 4.13: Percentage of M1 macrophages as defined by $CD80^+/CCR2^+$ cells. Cells were treated as described in the legend to Fig. 4.12 above. Bars represent the mean (±SEM) of $CD80^+/CCR2^+$cells from 6 independent experiments. °p<0.05 *vs* LPS.

To further characterize the effect of curcumin analogues on macrophage activation we investigated the modulation of M2 markers CD163 and CD206 after activation. Fig. 4.14A shows that, under basal conditions, glucocorticoid treatment significantly increased the percentages of $CD206^+/CD163^+$ subpopulations with respect to untreated macrophages (8.8±2.2 *vs* 3.4±0.9%, *p<0.05, n=3), as previously published by our group (Tedesco et al., 2015). Pre-treatment with GG9 did not affect the percentages of $CD206^+/CD163^+$ cells after 24h (Fig. 4.14A). Fig. 14B shows that dexa treatment prevented the decrease in M2 macrophages, as measured taking into account the fraction of $CD206^+/CD163^+$ cells, induced by pro-

inflammatory activation (5.9±2.0 *vs* 1.1±0.4%, n=5). Treatment with the curcumin analogue GG9 did the same through a significant effect in counteracting the LPS-induced down-regulation of $CD206^+/CD163^+$cells (3.4±1.0 *vs* 1.1±0.4%, n=5, Fig. 4.14B). CLI095 again had a similar and significant effect upon LPS activation (3.4±0.8 *vs* 1.1±0.4%, °p<0.05, n=5).

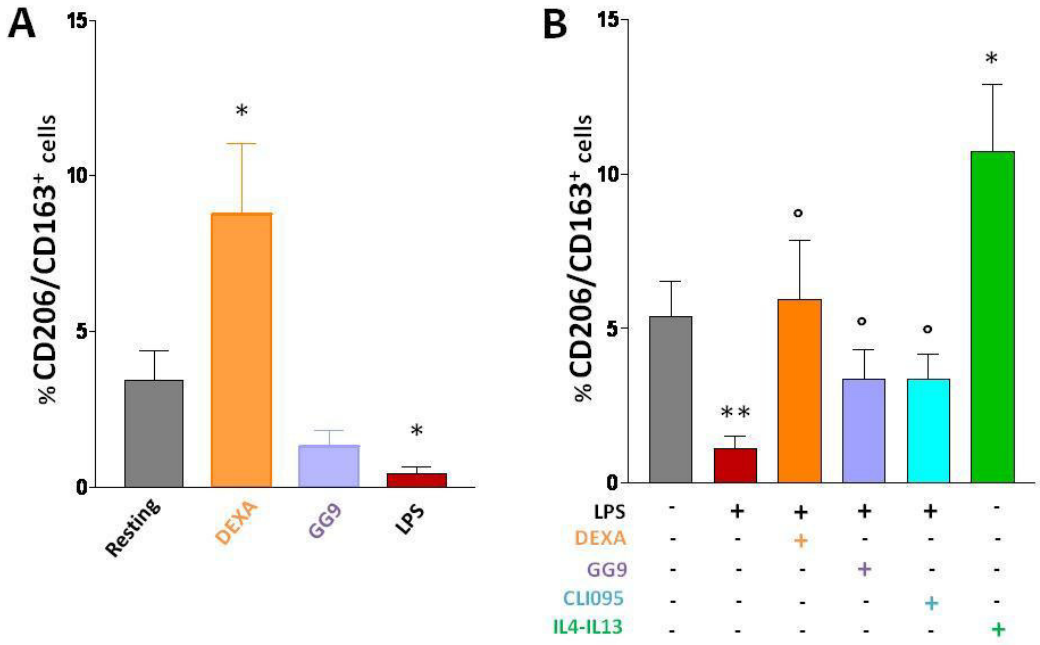

Figure 4.14: Percentage of M2 macrophages as defined by $CD206^+/CD163^+$ cells. Cells were treated as described in the legend to Fig. 4.12 above. Bars represent the mean (±SEM) of $CD206^+/CD163^+$cells in basal condition (panel A) and $CD206^+/CD163^+$cells with curcumin analogues pre-treatment and LPS activation (panel B) from 3-5 independent experiments. *p<0.05 and **p<0.005 *vs* resting, °p<0.05 *vs* LPS.

4.3.3 Effect of curcumin analogues upon NF-κB activation

We then assessed whether curcumin analogues modulated IκB-α expression profiles, as an index of NF-κB activation. After 30 min incubation with LPS (M1), IκB-α expression was significantly down-regulated by 40% compared with resting macrophages (Fig. 4.15). In particular, 30 min pre-treatment with GG9 did not alter the protein level with respect to LPS, as shown in Fig. 15, whereas curcumin, GG6 and CLI095 significantly reverted NF-κB activation (GG6 0.94±0.12, curcumin 0.83±0.08, CLI095 1.0±0.09 *vs.* LPS 0.6±0.04, p<0.05, n=3; Fig. 4.15).

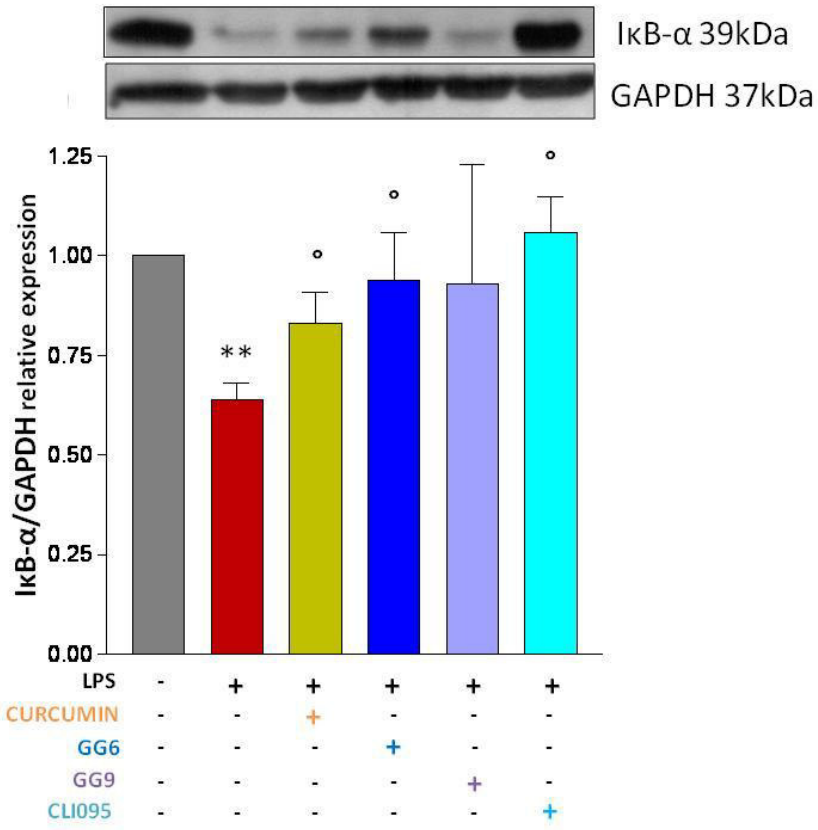

Figure 4.15: IκB-α expression in CSF-1-driven macrophages. Total protein extracts from resting, untreated M1 and curcumin analogue-pretreated macrophages showed a significant down-regulation of IκB-α after 30 min LPS incubation. GADPH served as loading control. Bars represent the mean (±SEM) of 3 independent experiments. Results from a representative immunoblot are shown. **p<0.0005 *vs* resting, °p<0.05 *vs* LPS.

4.3.4 Effects of curcumin analogues and CLIO95 on IL-1β production in cultured macrophages

We measured the percentage of CSF-1-derived macrophages expressing intracellular IL-1β and investigated whether GG9 or CLI095 pre-treatment could influence this process. As shown in Fig. 4.16B, a small fraction of IL-1β$^+$ cells (1.4±0.1%) was detected under basal conditions. Following 24-h incubation with LPS, the fraction of cells staining for cell-bound IL-1β was significantly increased (19.8±5 *vs* 1.4±0.1% IL-1β$^+$ cells *vs.* unstimulated, p<0.01, n=4, Fig.4. 16B). Compared with M1 cells, 30 min pre-treatment with either GG9 or CLI095

significantly decreased the percentage of IL-1β^{+}cells (6.1±2.6% GG9, 1.6±0.4% CLI095 *vs* 20.7±7 % LPS, p<0.05, n=4, Fig. 4.16B).

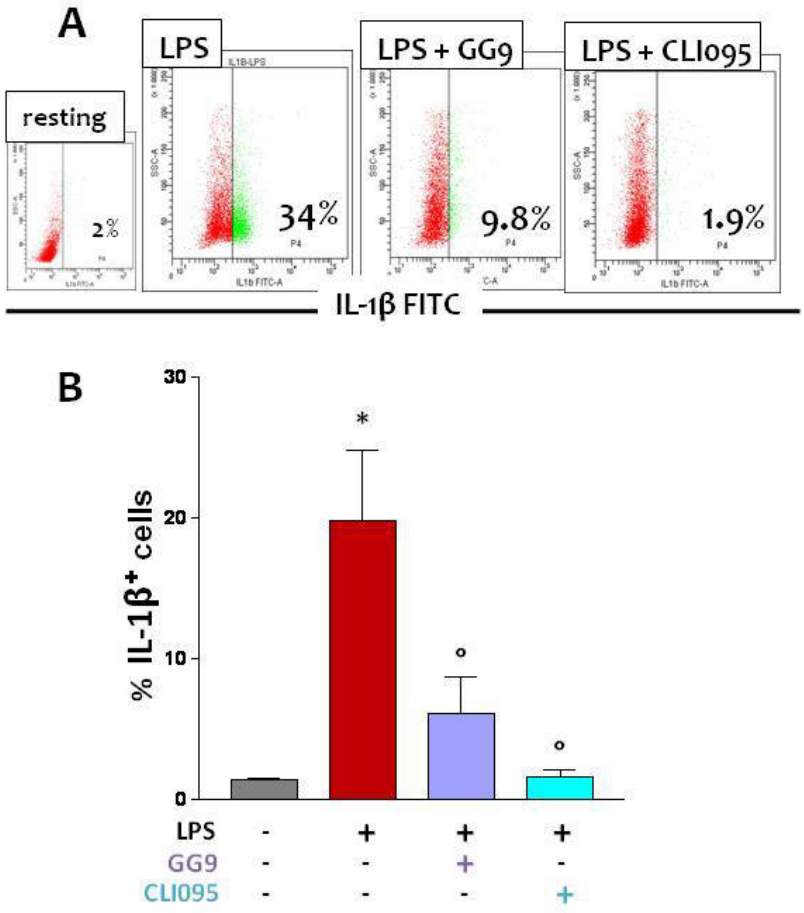

Figure 4.16: Effect of GG9 and CLI095 on CSF-1 derived macrophage cytokine expression. After differentiation, macrophages were pre-treated with GG9 or CLI095 for 30 min, and then incubated with LPS for 24h at 37°C in the presence of brefeldin (10 µM) to block cytokine secretion. Prior to flow cytometry analysis fixed/permeabilized cells were stained with a FITC-anti IL-1β antibody. Bar graph (B) represents the mean (±SEM) of 4 independent experiments, and fluorescence quantification dot plots (A) are from a representative experiment. *p<0.01 *vs* resting, °p<0.05 *vs* LPS.

To further explore the effects of curcumin and its analogues on macrophage cell activation, the pro-inflammatory cytokine IL-1β was quantified both in the protein lysate and in the medium. All these experiments were performed in FBS-free RPMI. Although the baseline level was very low, 24h of LPS stimulation significantly increased the production of intracellular IL-1β (5302±1342 *vs* 160±84 pg/ml, p<0.01, n=3; Fig.4.17A). Curcumin and GG6 did not affect the levels of intracellular cytokine

but 30-min pre-treatment with GG9 and CLI095 significantly blocked LPS-induced IL-1β production (918±257 pg/ml GG9 and 356±282 CLI095 *vs* 160±84 pg/ml, p<0.05, n=3; Fig. 4.17A). In untreated samples the basal level of IL-1β released in the medium was not detectable (ND). In contrast, 24-h LPS activation induced a marked release of the pro-inflammatory cytokine by macrophages (740±210 pg/ml, p<0.05, n=2; Fig. 4.17B). Curcumin and GG6 did not affect the cytokine release whereas 30 min GG9 pretreatment significantly inhibited it (101±101 *vs* 740±210 pg/ml, p<0.05, n=2; Fig. 4.17B). IL-1β after CLI095 pretreatment and LPS stimulation was not detectable (Fig. 4.17B).

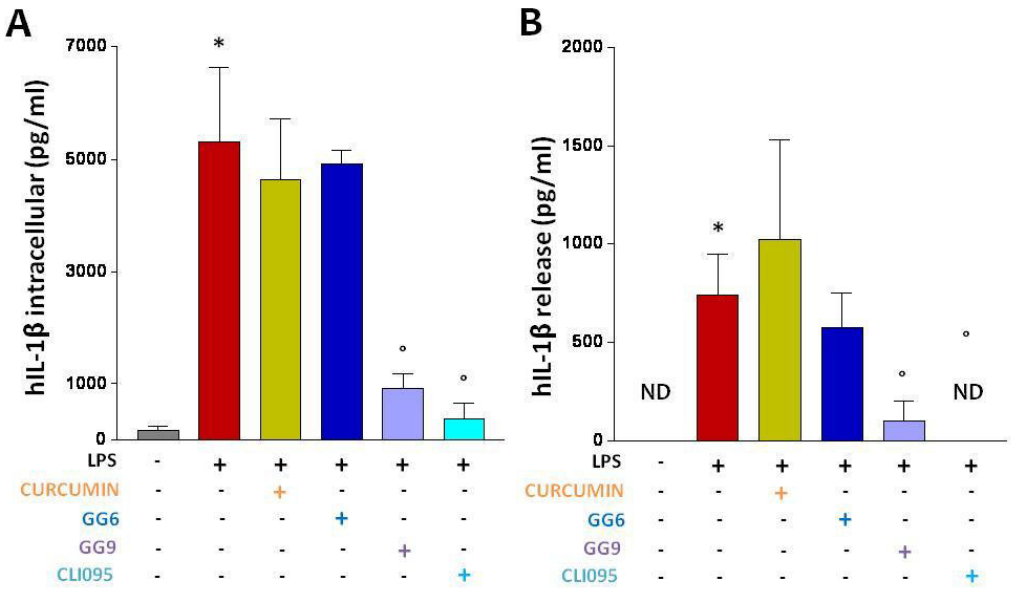

Figure 4.17: Assay of intracellular (panel A) and released (panel B) IL-1β from CSF-1 derived macrophages. After differentiation, macrophages were pre-treated with curcumin, GG6, GG9 or CLI095 for 30 min, and then incubated with LPS for 24h at 37°C in FBS-free RPMI. After incubation, culture medium and cell lysate samples were harvested for IL-1β analysis by ELISA. Bar graph of panel A represents the mean (±SEM) of 3 independent experiments, and panel B represents the mean (±SEM) of 2 independent experiments. *p<0.05 *vs* resting, °p<0.05 *vs* LPS.

5. Discussion

The turmeric plant is an herb belonging to the ginger family and has been used throughout history as a dietary spice and coloring agent in Indian and Chinese cuisines. The rhizome part of the plant has also been used for centuries in Indian and Chinese traditional medicines but the first documented case of its use as a drug was only in 1937, when it was used to treat biliary disease (Akbik et al., 2014). The remarkable healing properties and safety of curcumin motivated research groups all over the world to study this natural product. Curcumin was shown to have many biological activities including antioxidant, cardio- and neuroprotective, antidiabetic, antimicrobial, antimalarial, anti-human immunodeficiency virus (HIV), thrombosuppressive, antitumour and chemopreventive actions in a variety of experimental settings (Oliveira et al., 2015). Due to a vast number of biological targets, curcumin has achieved the potential therapeutic interest to be included in treatment protocols of immune-related, metabolic diseases and cancer. Over the past few years, many review articles have been published on curcumin biological activities (Priyadarsini et al., 2003; Joe et al., 2004; Maheshwari et al., 2006; Menon and Sudherr, 2007; Ghosh et al., 2015). Several studies suggest that curcumin has a diverse range of molecular targets, supporting the view that this compound influences a variety of biochemical and molecular cascades. Most studies suggest that the biological effects of curcumin are mainly due to its ability to either bind directly to various proteins and regulatory enzymes or modulate the intracellular redox state (Priyadarsini et al., 2003; Menon and Sudherr, 2007). Modulation of cellular redox homeostasis exerts an indirect but more global effect on a number of cellular processes, since several critical transcription factors are sensitive to even minor fluctuations in the cell redox *milieu*. The intricate mechanism of action of curcumin involves various biological targets via transcription factors (i.e. NF-κB, NF-AT, AP-1, signal transducers and activator of transcription (STAT) and p53) as well as kinases, cytokines release, and receptors found on different immune cell type. the above mechanisms control cell cycle, differentiation, stress response and other physiological processes. Although curcumin does not have a drug profile yet, the safety of oral curcumin (12 g/day), which is much higher than its regular intake as a food supplement, has been established by regulatory agencies (Lao et al., 2006). In response to the growing interest in curcumin and its biological activities, several

clinical trials have addressed the safety, pharmacokinetics and efficacy in humans. These trials have tested specific and promising biological activities of curcumin as shown by *in vitro* and preclinical assays (clinicaltrials.gov; Oliveira et al., 2015). However, there are certain limitations concerning the use of curcumin as a drug. Due to its insolubility in water, curcumin has very poor bioavailability, its cellular uptake is slow and it gets metabolized very fast once inside the cell. Therefore, it requires repeated oral doses in order to achieve significant intracellular concentrations for any physiological effects. To address these limitations, a large number of curcumin analogues with improved uptake, metabolism and activity have been designed (Srivastava et al., 2011).

Curcumin appears to affect innate and adaptive immunity, especially in pathological conditions, by effectively modulating the function of T cells, B cells, DCs, monocytes, macrophages and neutrophils (Srivastava et al., 2011). Several reports have highlighted the anti-inflammatory action of curcumin and its potential role in the treatment of immune cell-related diseases. Few studies investigated the effect of curcumin and its analogues on macrophage activation. Mercanti et al. (2014) and Tocharus et al. (2012) studied the effects of curcumin on mouse microglia activation inhibiting the NO production induced by LPS and the IL-1β, IL-6 and TNF-α release in the medium. Another study demonstrated that curcumin induces macrophage M2 polarization by increasing the production of IL-4 and/or IL-13 and STAT6-dependent manner (Gao et al., 2015), suggesting that curcumin and its anologues represent promising lead compounds targeting immune cells activation. Therefore, one specific aim of the present work was to test the potential of curcumin analogues as modulators of human macrophage function.

Because recent advances in macrophage development and functional diversity indicate a multidimensional concept of macrophage ontogeny, activation and function (Ginhoux et al., 2015), research in pharmacological targeting of macrophage function is challenging. The diversity of terminology and inconsistent use of markers to describe macrophage activation impedes reaching a consensus in this research field. In fact, mononuclear phagocytes are an essential element in the orchestration and expression of innate immunity and adaptive immune responses.

It has been demonstrated that, in response to signals derived from microbes, damaged tissues or activated lymphocytes, monocyte/macrophages undergo a reprogramming which leads to the emergence of a spectrum of distinct functional phenotypes (Sica and Mantovani, 2012). According to the current framework, macrophages can be polarized into classically (M1) or alternatively (M2) activated cells, representing two polar extremes of signals computed by macrophages. The existence of at least two phenotypically and functionally distinct subsets of macrophages as well as circulating monocytes has been demonstrated in both humans and mice (Mosser and Edwards, 2008; Mantovani et al., 2009; Motwani and Gilroy, 2015). Because nature of polarizing agents and exposure time appear to be crucial, a panel of leading immunologists recently published experimental guidelines for macrophage activation and polarization (Murray et al., 2014).

Thus, when we set out to explore the effect of curcumin on macrophage polarization, the first key step was to set up a model of human monocyte-derived macrophages. In the literature a variety of protocols are described to isolate blood circulating monocytes and promote monocyte-to-macrophage differentiation, each with its own pros and cons. In particular, macrophages can be obtained from immortalized cell lines (e.g., THP-1) or by purifying blood monocytes, either through magnetic cell sorting using specific CD14-labeled magnetic beads (Martinez et al., 2013) or by density gradient centrifugation. Our published protocol involved: (i) monocyte isolation by Ficoll stratification, and (ii) spontaneous FBS-driven differentiation with no additional growth factors in the medium (Tedesco et al., 2015). One limitation of this procedure, however, is that the FBS-driven macrophage population includes 20-30% of $CD3^+$ cells 24 h after seeding that drop down to 10-15% at the end of differentiation. Our improved method as described herein is based on two gradient centrifugations upon polymers, first on Ficoll-paque and next on Percoll. Pure monocytes obtained using this method need to be cultured with CSF-1 in the medium to allow differentiation into macrophages. We then monitored and compared the differentiation period (from monocytes to macrophages in 7 days) and the purity of this CSF-1 driven culture. At 24 h from seeding, monocytes cultured by the CSF-1-driven protocol had no accompanying

$CD3^+$ cells. After 7 days FBS-driven $CD3^+$percentage decreased and reached the 15% as reported by Eligini et al (2012), as noted above, but CSF-1-driven $CD3^+$cells remained 0%. Therefore, our improved CSF-1-driven protocol generated diverse macrophage subpopulations with a virtually complete lack of $CD3^+$ cells. During the 7 days' differentiation with both protocols macrophages increased their size and acquired different shape and morphology, showing mainly two dominant and distinct morphotypes: spindle/elongated and round-/"fried-egg" shaped, which routinely occurred in resting cultures (Eligini et al., 2012; Vogel et al., 2014). The presence of two distinct macrophage subsets was confirmed by flow cytometry as a differential distribution on the forward scatter (FS) parameter, which is indicative of the cell size. In line with our results, Eligini and colleagues (2012) demonstrated the presence of two dominant monocyte-derived macrophages morphotypes under basal conditions. In particular, they highlighted the presence of about 50% spindle-shaped cells that display an M1-like phenotype, and about 50% of round-shaped cells that display an M2-like phenotype utilizing laser capture microscopy followed by RT-PCR for characterization of specific immunophenotypes. Recently Vogel et al. (2014) confirmed these findings. At the end of differentiation resting macrophages (M0) from both protocols showed lower levels of $CD80^+$/$CCR2^+$ and higher fractions of $CD206^+$/$CD163^+$ cell subpopulations, indicating that in resting state macrophages present a main "M2-like" phenotype. Hence the CSF-1 driven protocol allowed us to obtain a pure monocytes population and, after differentiation, a more homogeneous macrophage population.

As opposed to other studies, we exposed macrophages to M1- and M2-activating agents only after these cells were fully differentiated and not during the differentiation period. On one hand, during inflammation monocytes will enter inflamed tissues and will be exposed to TLR-ligands or cytokines during their differentiation. However, tissue-resident macrophages, which have recently been shown to be self-renewed (Schulz et al, 2012; Okabe and Medzhitov, 2015), will in a lot of cases be exposed to these agents only after their differentiation. As a potential future research question, it would be very interesting to compare a similar cytokine exposure to monocytes and to differentiated macrophages, such as 3 days

of exposure during differentiation and then 3 days of exposure after differentiation. Along the same lines, it would be interesting to sort spontaneously differentiated M2 cells and then expose them to M1-triggers to see if they can switch from phenotype or not or if M2 cells that were exposed to IL-4/IL-13 during their differentiation could switch easily to M1 or are more locked in an M2 state.

In the present work, we specifically polarized monocyte-derived macrophages with LPS to induce the M1 phenotype, or with IL-4/IL-13 to obtain the M2 phenotype (24-h incubation after differentiation period in both cases). We observed that macrophage polarized activation toward M1 or M2 immunophenotypes were accompanied by specific changes in cell morphology compared with resting state. In particular, we observed that M1 macrophages were enriched in the long, spindle-shaped morphotype, while M2 macrophages were largely round-shaped. Similar observations were made by Eligini et al. (2012) and Vogel et al. (2014). As noted above, M1 and M2 phenotypes can be identified by a wide range of surface markers (CD cluster of differentiation, as well as cytokine and chemokine receptors) which are distinct between human and mouse (Auffray at al., 2009; Mantovani et al., 2009; Murray et al., 2014). Unfortunately, a gold standard classification of phenotype markers is still lacking, although Murray and colleagues (2014) tried to address the problem. In particular, the surface markers most commonly used to identify classical M1 macrophages are the T-cell co-stimulatory molecules CD80 and CD86, and the monocyte chemoattractant protein-1 receptor CCR2, while the mannose scavenger receptor CD206 together with CD163 (haemoglobin-heptoglobin receptor) are often used to identify the M2 subset. More recent studies used additional surface markers to better distinguish macrophage subsets. In particular, Vogel et al. (2014) investigated novel M1-associated (CD40, CXCL11 and CCR7) as well as M2-associated (stabilin-1, CD180 and TREM2) cell surface markers, and Ambarus and colleagues (2012a) validated specific phenotypic markers for *in vitro* polarized human macrophages, such as CD80 and CD64 for IFNγ-activated M1 macrophages and CD200R for IL-4-activated M2a macrophages. Gordon and colleagues (2014) suggested CD169 as a new and promising M1 marker; Martinez et al (2013) performed extensive analysis of mouse and human

alternative macrophage activation, and found a set of highly conserved genes that were regulated by IL-4 including transglutaminase (TGM)-2. Taken together, these findings suggest that any selection of phenotypic markers is certainly non-exhaustive and strictly dependent to the differentiation protocol as well as the activating agents used to induce M1/M2 immunophenotypes.

We selected CD80 and CCR2 as M1 markers, and CD206, CD163 as markers of the M2 immunophenotype. CD80 is a co-regulatory receptor expressed on the surface of antigen presenting cells (Dakappagari et al., 2012). Macrophage subpopulations have been reported to express high levels of CD80 and CD86; these macrophages can present antigens to T cells, thus promoting the inflammatory immune response. Jaguin et al. (2013) demonstrated that expression of CD80, which is a strong membrane marker of M1 polarization, significantly increased after 24-h LPS/IFNγ polarization of M-CSF/CSF-1–differentiated human macrophages. In addition, Stöger et al. (2012) demonstrated the prevalence of CD86-expressing M1 macrophages in atherosclerotic plaques prone to rupture. We observed a significant increase in the fraction of $CD80^{+}$ spontaneously differentiated macrophages after M1 polarization compared with resting macrophages. These results are in line with those of Ambarus and colleagues (2012), who demonstrated the up-regulation of CD80 in human macrophages treated with IFN-γ or TNF-α for 4 or 7 days starting at the beginning of the maturation protocol. CCR2, also known as the receptor for MCP-1/CCL2, is widely accepted as an M1 macrophage marker (Mantovani et al., 2009). Interestingly, it is also expressed on circulating monocytes, and has long been used to identify classical/M1 $Ly6C^{high}$ $CX3CR1^{low}CCR2^{+}$ monocytes in mice (Fadini et al., 2013). We found that the number of $CCR2^{+}$ macrophage was already high in the resting state (M0) and did not further increase after LPS/IFNγ treatment, which limited the relevance of CCR2 to our model. Overall, these data suggest that 24h activation with LPS of CSF-1 differentiated macrophages is able to enhance the pro-inflammatory macrophage immunophenotype, specifically by increasing the fraction of $CD80^{+}$, $CD80^{+}/CCR2^{+}$ cells. The mannose receptor CD206 is a well established M2 marker, as well as CD163 (Mantovani et al., 2009; Toniolo et al., 2014; Vogel et al., 2014; Chinetti-Gbaguidi et al., 2015). When characterizing the

M2 immunophenotype, we demonstrated high levels of $CD206^+$ and $CD163^+$ cells in resting conditions. Interestingly, after LPS activation, the percentage of the M2 immunophenotype significantly decreased independently from the marker used for M2 characterization. These results demonstrated that pro-inflammatory stimuli are able to enhance the M1 macrophage subset, as well as attenuate the M2 phenotype. This also indicates that a pro-inflammatory microenvironment causes an M2-to-M1 immunophenotype switch and confirms the plasticity of human macrophages, which are able to adapt their phenotype and functions according to specific microenvironmental signals. Accordingly, studies of adipose tissue macrophages in a mildly obese mouse model showed that the M1 subset increases concomitantly with a reduction in M2 macrophages, due to enhanced secretion of chemoattractant molecules and pro-inflammatory cytokines (Lumeng et al., 2007; Kraakman et al., 2014).

We extended our findings of morphology and macrophage activation as described above with data of specific surface marker expression in the human monocyte cell line THP-1, in a condition of total absence of $CD3^+$ cells. One advantage of using macrophage cell lines is increased homogeneity and purity as compared to primary cells. THP-1 cells have been proposed as a simplified model to study monocyte–macrophage polarization (Qin et al., 2012). However, new data redefine tissue macrophages as a layered system composed of resident macrophages originating mostly from yolk-sac progenitor cells and transitory myeloid cells that originate and renew from bone marrow hematopoietic stem cells (Gomez-Perdiguero and Geissmann, 2015). Therefore, we and others feel that blood-derived macrophages represent a more accurate (and complex) model of macrophage heterogeneity that is more suitable to investigate macrophage function *in vitro* and *ex vivo*.

We further defined macrophages subsets after polarization in terms of gene expression and cytokine production. Several genes were previously identified as M1 or M2 markers (Mantovani et al., 2013; Tedesco et al., 2015). The pro-inflammatory cytokines TNF-α, IL-6 and IL-1β are critical mediators of the acute phase response, and are potently induced after LPS or IFN-γ treatment. We observed a higher mRNA expression of TNF-α and IL-1β in M1 than in non-polarized (M0) or M2

macrophages. In particular, the mRNAs encoding these cytokines accumulated with a different time course, e.g. TNF-α mRNA peaked at 6h while IL-1β reached the highest expression level after 48h. It is conceivable that macrophages respond to pro-inflammatory stimuli by producing TNF-α, which in turn induces IL-1β gene expression, thus fortifying the concept that macrophage activation encompasses a quantifiable and temporally dynamic process (Tarique et al. 2015). IL-10 was previously described as a key marker for the M2 immunophenotype (Mantovani et al., 2013) as well as an M2-polarizing agent (Mantovani et al., 2004). Several studies are consistent in defining M2 anti-inflammatory macrophages as cells releasing high amounts of this cytokine (Mantovani et al., 2013). In addition, differences in IL-10 expression in lean (higher expression) compared with obese (lower expression) mouse adipose tissue macrophages (ATMs) have been reported, thus implying an important role of this cytokine as a homeostatic regulator in insulin sensitivity (Kammoun et al., 2014). Unexpectedly, we found that IL-10 mRNA levels were significantly increased in M1 (LPS) but not in M2 (IL-4/IL-13) activated cells, both after 6 and 48 h (Tedesco et al., 2015). Nevertheless, several studies are consistent with our findings, demonstrating either increased IL-10 release into the culture medium after LPS stimulation (Ambarus et al., 2012b), LPS-induced IL-10 intracellular accumulation in PBMCs (Muris et al., 2012) or increased IL-10 mRNA levels in human M-CSF-generated macrophages after M1 polarization (Jaguin et al., 2013). We hypothesize that the LPS stimulus is able to induce a typical anti-inflammatory cytokine, such as IL-10, which probably triggers M2 macrophage polarization via more complex and long-term feedback mechanisms. In fact, the rapid peak (6h) in IL-10 mRNA levels suggests a possible role of this LPS-responsive cytokine in a M1-to-M2 transition involved in the resolution of acute inflammatory events (Couper et al., 2008).

Furthermore, we analyzed cytokines released into the culture medium of M1 and M2 activated macrophages by Luminex technology. We looked at the production of a panel of 50 cytokines and metabolites in order to correlate the modulation of macrophage immunophenotypes with their function. In agreement with mRNA expression data, we found increased TNF-α, IL-1β and IL-10 extracellular protein

accumulation after incubation with LPS in CSF-1-derived macrophages, in addition to IL-6, VEGF and IP-10 (also known as CXCL10 or IFN-γ induced protein-10). M2 activated macrophages appear to be the most vigorous producers of IL-4 and CCL22, also known as macrophage derived chemokine (MDC; Vulcano et al., 2001). In agreement with our data, IL-4 and IL-13 have been reported to induce CCL22 production in monocytes, monocyte-derived macrophages, natural killer (NK) cells and DCs (Vulcano et al., 2001). CCL22 expression and secretion was also found to be increased in M2 when compared with M0 and M1 macrophages (Jaguin et al., 2013; Toniolo et al., 2014).

The second specific aim of this thesis was to evaluate the impact of curcumin and its analogues on macrophage immunophenotypes and function. So far few studies addressed if and how specific pharmacological agents affect human macrophage immunophenotypes (Bouhlel et al., 2007, Van der Meij et al., 2013). In particular, the effects of glucocorticoids were explored in mouse bone marrow-derived macrophages (Yang et al., 2012) and in human circulating monocytes (Ehrchen et al., 2007; Vallelian et al., 2010). Recently, dexamethasone was shown to induce expression of specific human macrophage phenotypic markers according to activation protocol and treatment duration including CD163 (Ambarus et al., 2012a; Tang et al., 2013). Glucocorticoids have been also found to induce a particular mouse macrophages M2 subset, called M2c (Martinez et al., 2008). A recent study from our group demonstrate that 17β-estradiol affects macrophage polarization and function by preventing LPS effects on the M2 immunophenotype and cytokine production (Toniolo et al., 2014). The literature on the potential of natural compounds to modulate human macrophage activation and polarization is quite limited. In particular, although anti-inflammatory effects of curcumin have been reported in a variety of experimental models (Aggarwal and Harikumar, 2009; Shehzad et al., 2013), the possibility that curcumin and/or analogues thereof affect human macrophage activation has not been explored in much detail. It is worth noting that all above studies have been performed in murine macrophages or THP-1 cell line. We decided to investigate these aspects using dexamethasone and CLI095 as positive controls using our model of human CSF-1-derived macrophages.

It has been shown that curcumin regulates diverse molecular targets implicated in inflammation. Specifically, curcumin inhibits inflammatory cytokines such as TNF-α, IL-1, IL-6, IL-8, mitogen-activated protein kinase (MAPK), and suppresses inducible nitric oxide synthase (iNOS), COX-2 and lipoxygenase (LOX) in a variety of cancer cells (Priyanka et al., 2014; Liu et al., 2015). In this regard, our hypothesis is that curcumin is mainly acting as an inhibitor of LPS activation, especially on the expression of M1 markers (such as CD80) that are modulated via the NF-κB pathway (Lien and Golembock, 2003). Our data clearly show that the curcumin analogue GG9 was able to prevent the up-regulation of CD80 expression induced by LPS activation (Fig. 4.12 panel A and B), thereby modulating M1 polarization. This effect was also observed for the $CD80^{+}/CCR2^{+}$ population, although statistical significance was not achieved. In the literature curcumin is reported to affect M2 activation: in particular, Chen and colleagues (2014) showed that curcumin not only directly induces the polarization of macrophages to M2 phenotype, but also promotes a switch from M1 to M2 phenotype in RAW264.7 macrophages. More recently, Gao et al. (2015) demonstrated that curcumin induces M2 polarization of RAW264.7 cells by increasing the production of IL-4 and/or IL-13 in a STAT6-dependent manner. In our model of CSF-1-derived human macrophages, treatment with GG9 significantly prevented LPS-induced down-regulation of M2 markers, thereby acting as an anti-inflammatory agent. In contrast with Gao's work above, no effect on the M2 markers could be seen with GG9 alone, while dexamethasone treatment in M0 or activated M2 macrophages enhanced $CD206^{+}/CD163^{+}$ macrophage subsets, consistently with findings from different experimental models (Fig. 4.14; Ambarus et al., 2012b; Heasman et al., 2004, Tang et al. 2013; Tedesco et al., 2014).

The LPS-induced production of inflammatory mediators is linked to a series of intracellular signaling pathways ultimately resulting in activation of NF-κB, which regulates the expression of a variety of target genes, including those encoding cytokines. Singh and Aggarwal (1995) were the first to demonstrate that curcumin is a potent blocker of NF-κB activation induced by different inflammatory stimuli. Subsequently, they showed that curcumin blocks NF-κB activation through inhibition of IκB-α kinase and Akt (Aggarwal et al., 2005), thus resulting in the

suppression of NF-κB–dependent gene products (Aggarwal and Harikumar, 2009). More recently other studies showed that NF-κB nuclear translocation is mediated at least in part by direct inhibition of expression and/or activation of TLR2 or TLR4, or their associated signaling proteins (Youn et al., 2006; Lubbad et al., 2009; Zhou et al., 2015; Wang et al., 2015). In particular, Youn et al. (2006) described in detail the molecular mechanisms by which curcumin acts on NF-κB pathway: the compound inhibits LPS-induced TLR4 dimerization, and its α,β-unsaturated carbonyl group can react with –SH group in cysteine in the activation loop of IKK-β, resulting in inhibition of IKKβ kinase activity. Gradisar and colleagues (2007) proposed a different interaction: within its structure, curcumin binds at submicromolar affinity through its 3-(4-hydroxyphenyl) acrylaldehyde moiety to MD2, a protein that associates with TLR4 and confers responsiveness to LPS, thus providing a link between the receptor and LPS signaling. According to Gradinsar, curcumin may compete with LPS for the same binding site on MD2, thus resulting in the pharmacological outcomes of suppression of LPS inflammatory cascade. More recently, Zhou et al. (2015) also described that the turmeric compound decreased TLR4 expression. In particular they found out that TLR4 small interfering RNA transfection in combination with p-JNK, p-ERK, and p-p38 inhibition reduced the effect of curcumin on the polarization of THP1-derived macrophages (Zhou et al., 2015). Furthermore, Buhrmann et al. (2011) demonstrated that curcumin suppresses IL-1β-induced NF-κB activation and nuclear translocation as well as IL-1β induced phosphatidylinositol 3-kinase (PI3K/Akt) activation through decreased phosphorylation and degradation of IκB-α. We assessed whether curcumin analogues modulated IκB-α expression profiles as an index of NF-κB activation in our model (Fig. 4.15). The curcumin analogue GG9 did not alter IκB-α protein level with respect to LPS whereas treatment with curcumin, GG6 or CLI095 significantly prevented NF-κB activation. More experiments are required to further investigate the effect of GG9, which appears to interfere with the NF-κB pathway. Recently Mercanti et al. (2014) demonstrated that non-cytotoxic concentrations of phosphatidylserine and curcumin significantly inhibit the LPS-induced release of pro-inflammatory IL-1β, IL-6 and TNF-α in primary rat microglia. As for studies in

human cell systems, Abe et al. (1999) first demonstrated that curcumin inhibits inflammatory cytokines production in human peripheral blood monocytes.

In order to evaluate whether curcumin affects human monocyte-macrophage function along with immunophenotypes, we invesigated the effects of GG9 on cytokine production in CSF-1-derived macrophages (Fig. 4.16 and 4.17). Dexamethasone and CLI095 were again used as positive controls. GG9 appeared to be active on both cell-bound and intra-/extracellular IL-1β, as this curcumin analogue was able to significantly block cell-bound IL-1β production as well as that in cell lysate and in the culture medium. By contrast, curcumin and GG6 did not affect the levels of intra- and extracellular IL-1β, suggesting a different interaction of those molecules with the receptor at a structural level. It is important to underline that IL-1β production by CSF-1–derived macrophages was very difficult to assess because IL-1β occurs in cells at two different stages of maturation: pro-IL-1β and IL-1β (Ferrari et al., 1997). Seen that the antibodies used are able to bind both forms, the experimental set up was complicated. As a potential future research question, it would be interesting to investigate how curcumin and its analogues modulate the release of other cytokines, both with pro-inflammatory (TNF-α) and anti-inflammatory (IL-10, CCL22, IL-4) activity, and if or how long-term stimulation (3-7 days) affect macrophage M2 polarization, thus acting like dexamethasone or E2 (Tedesco et al., 2015; Toniolo et al., 2014).

Taken together, these results provide the basis to support the central hypothesis of this project that natural compounds could affect monocyte-macrophage immunophenotypes, in particular by acting on LPS activation through NF-κB pathway. We found that curcumin analogues were able to prevent the down-regulation of M2 markers and the up-regulation of M1 markers, and to block secretion of the pro-inflammatory cytokine IL-1β following LPS activation, suggesting that these compounds impact on macrophage function *in vitro*. On a molecular level, in agreement with previous studies, curcumin analogues are able to block the NF-κB signaling pathway, probably acting at different levels on TLR4-MD2 interaction and IKKβ kinase activity (Youn et al., 2006; Gradisar et al., 2007).

The possibility to promote a macrophage protective phenotype has become a therapeutic goal in the treatment of inflammatory conditions, and the identification of factors that control cell activation is currently an area of active research. Overall, this project's output suggests that polarized activation protocols shape the functional status of macrophages and are critical to investigate pharmacological macrophage targeting. The present findings suggest that curcumin and its analogues represent promising lead compounds targeting immune cells activation.

6. References

Abe Y, Hashimoto S, Horie T. Curcumin inhibition of inflammatory cytokine production by human peripheral blood monocytes and alveolar macrophages. *Pharmacol Res*. **1999** Jan; 39(1):41-7

Aggarwal BB, Shishodia S, Takada Y, Banerjee S, Newman RA, Bueso-Ramos CE, Price JE. Curcumin suppresses the paclitaxel-induced nuclear factor-kappaB pathway in breast cancer cells and inhibits lung metastasis of human breast cancer in nude mice. *Clin Cancer Res*. **2005** Oct; 11(20):7490-8

Aggarwal BB, Harikumar KB. Potential therapeutic effects of curcumin, the anti-inflammatory agent, against neurodegenerative, cardiovascular, pulmonary, metabolic, autoimmune and neoplastic diseases. *Int J Biochem Cell Biol*. **2009** Jan; 41(1):40-59

Akbik D, Ghadiri M, Chrzanowski W, Rohanizadeh R. Curcumin as a wound healing agent. *Life Sci*. **2014** Oct; 116(1):1-7

Alok A, Singh ID, Singh S, Kishore M, Jha PC. Curcumin – pharmacological actions and its role in oral submucous fibrosis: a review. *J Clin Diagn Res*. **2015** Oct; 9(10):ZE01-3

Ambarus CA, Krausz S, van Eijk M, Hamann J, Radstake TR, Reedquist KA, Tak PP, Baeten DL. Systematic validation of specific phenotypic markers for in vitro polarized human macrophages. *J Immunol Methods*. **2012a**; 375: 196-206

Ambarus CA, Santegoets KC, van Bon L, Wenink MH, Tak PP, Radstake TR, Baeten DL. Soluble immune complexes shift the TLR-induced cytokine production of distinct polarized human macrophage subsets towards IL-10. *PLoS One* **2012b**; 7(4):e35994

Anand P, Thomas SG, Kunnumakkara AB, Sundaram C, Harikumar KB, Sung B,Tharakan ST, Misra K, Priyadarsini IK, Rajasekharan KN, Aggarwal BB. Biological activities of curcumin and its analogues (congeners) made by man and Mother Nature. *Biochem Pharmacol*. **2008** Dec;76(11):1590-611

Auffray C, Sieweke MH, Geissmann F. Blood monocytes: development, heterogeneity, and relationship with dendritic cells. *Annu Rev Immunol*. **2009**; 27:669-92

Banerjee S, Xie N, Cui H, Tan Z, Yang S, Icyuz M, Abraham E, Liu G. MicroRNA let-7c regulates macrophage polarization. *J Immunol*. **2013**; 190(12):6542-9

Bender AT, Ostenson CL, Giordano D, Beavo JA. Differentiation of human monocytes in vitro with granulocyte-macrophage colony-stimulating factor and macrophage colony-stimulating factor produces distinct changes in cGMP-phosphodiesterase expression. *Cell Signal*. **2004**; 16(3):365-74

Biswas SK, Mantovani A. Macrophage plasticity and interaction with lymphocyte subsets: cancer as a paradigm. *Nat Immunol.* **2010**; 11: 889–896

Bouhlel MA, Derudas B, Rigamonti E, Dièvart R, Brozek J, Haulon S, Zawadzki C, et al. PPARγ activation primes human monocytes into alternative M2 macrophages with anti-inflammatory properties. *Cell Metab*. **2007**; 6:137-143

Brancato SK, Albina JE. Wound macrophages as key regulators of repair: origin, phenotype, and function. *Am J Pathol*. **2011** Jan; 178(1):19-25

Buhrmann C, Mobasheri A, Busch F, Aldinger C, Stahlmann R, Montaseri A,Shakibaei M. Curcumin modulates nuclear factor κB (NF-κB)-mediated inflammation in human tenocytes in vitro – role of the phosphatidylinositol 3-kinase/Akt pathway. *J Biol Chem.* **2011** Aug; 286(32):28556-66

Chen F, Guo N, Cao G, Zhou J, Yuan Z. Molecular analysis of curcumin-induced polarization of murine RAW264.7 macrophages. *J Cardiovasc Pharmacol.* **2014** Jun; 63(6):544-52

Chinetti-Gbaguidi G, Colin S, Staels B. Macrophage subsets in atherosclerosis. *Nat. Rev Cardiol.* **2015**; 12(1), 10-7

Colin S, Chinetti-Gbaguidi G, Staels B. Macrophage phenotypes in atherosclerosis. *Immunol Rev.* **2014** Nov;262(1):153-66

Couper KN, Blount DG, and Riley EM. IL-10: the master regulator of immunity to infection. *J Immunol*. **2008**; 180: 5771-7

Dakappagari N, Ho SN, Gascoyne RD, Ranuio J, Weng AP, Tangri S. CD80 (B7.1) is expressed on both malignant B cells and nonmalignant stromal cells in non-Hodgkin lymphoma. *Cytometry B Clin Cytom*. **2012** Mar; 82(2):112-9

Davies LC, Taylor PR. Tissue-resident macrophages: then and now. *Immunology* **2015** Apr; 144(4):541-8

Delves PJ, Roitt IM. The immune system. *N Engl J Med.* **2000**; 343:37-49 and 108-17

Duewell P, Kono H, Rayner KJ, Sirois CM, Vladimer G, Bauernfeind FG, Abela ,GS, Franchi L, Nuñez G, Schnurr M, Espevik T, Lien E, Fitzgerald KA, Rock KL, Moore KJ, Wright SD, Hornung V, Latz E. NLRP3 inflammasomes are required for atherogenesis and activated by cholesterol crystals. *Nature* **2010** Apr; 464(7293):1357-61

Ehrchen J, Steinmüller L, Barczyk K, Tenbrock K, Nacken W, Eisenacher M, Nordhues U, Sorg C, Sunderkötter C, Roth J. Glucocorticoids induce differentiation of a specifically activated, anti-inflammatory subtype of human monocytes. *Blood* **2007** Feb; 109(3):1265-74

Eligini S, Crisci M, Bono E, Songia P, Tremoli E, Colombo GI, Colli S. Human monocyte-derived macrophages spontaneously differentiated in vitro show distinct phenotypes. *J Cell Physiol.* **2013** Jul; 228(7):1464-72

Fadini GP, de Kreutzenberg SV, Boscaro E, Albiero M, Cappellari R, Kränkel N, Landmesser U, Toniolo A, Bolego C, Cignarella A, Seeger F, Dimmeler S, Zeiher A, Agostini C, Avogaro A. An unbalanced monocyte polarisation in peripheral blood and bone

marrow of patients with type 2 diabetes has an impact on microangiopathy. *Diabetologia.* **2013** Aug; 56(8):1856-66

Fadini GP, Simoni F, Cappellari R, Vitturi N, Galasso S, Vigili de Kreutzenberg S, Previato L, Avogaro A. Pro-inflammatory monocyte-macrophage polarization imbalance in human hypercholesterolemia and atherosclerosis. *Atherosclerosis.* **2014** Dec; 237(2):805-8

Ferrari D, Chiozzi P, Falzoni S, Dal Susino M, Melchiorri L, Baricordi OR, Di Virgilio F. Extracellular ATP triggers IL-1 beta release by activating the purinergic P2Z receptor of human macrophages; *J Immunol.* **1997** Aug; 1;159(3):1451-8

Gao S, Zhou J, Liu N, Wang L, Gao Q, Wu Y, Zhao Q, Liu P, Wang S, Liu Y, GuoN, Shen Y, Wu Y, Yuan Z. Curcumin induces M2 macrophage polarization by secretion IL-4 and/or IL-13. *J Mol Cell Cardiol*. **2015** Aug; 85:131-9

Gautier EL, Jakubzick C, Randolph GJ. Regulation of the migration and survival of monocyte subsets by chemokine receptors and its relevance to atherosclerosis. *Arterioscler Thromb Vasc Biol*. **2009** Oct; 29(10):1412-8

Ginhoux F, Greter M, Leboeuf M, Nandi S, See P, Gokhan S, Mehler MF, Conway SJ, Ng LG, Stanley ER, Samokhvalov IM, Merad M. Fate mapping analysis reveals that adult microglia derive from primitive macrophages. *Science* **2010** Nov; 330(6005):841-5

Ginhoux F, Jung S. Monocytes and macrophages: developmental pathways and tissue homeostasis. *Nat Rev Immunol*. **2014** Jun; 14(6):392-404

Ginhoux F, Schultze JL, Murray PJ, Ochando J, Biswas SK. New insights into the multidimensional concept of macrophage ontogeny, activation and function. *Nat Immunol.* **2015** Dec; 17(1):34-40

Glass CK, Natoli G. Molecular control of activation and priming in macrophages. *Nat Immunol.* **2015** Dec; 17(1):26-33

Ghosh S, Banerjee S, Sil PC. The beneficial role of curcumin on inflammation, diabetes and neurodegenerative disease: a recent update. *Food Chem Toxicol*. **2015** Sep; 83:111-24

Gomez Perdiguero EG, Geissmann F. The development and maintenance of resident macrophages. *Nat Immunol*. **2015** Dec; 17(1):2-8

Gomez Perdiguero E, Klapproth K, Schulz C, Busch K, Azzoni E, Crozet L, Garner H, Trouillet C, de Bruijn MF, Geissmann F, Rodewald HR. Tissue-resident macrophages originate from yolk-sac-derived erythro-myeloid progenitors. *Nature* **2015** Feb; 518(7540):547-51

Gordon S, Taylor PR. Monocyte and macrophage heterogeneity. *Nat Rev Immunol*. **2005** Dec; 5(12):953-64

Gordon S, Plüddemann A, Martinez Estrada F. Macrophage heterogeneity in tissues: phenotypic diversity and functions. *Immunol Rev*. **2014** Nov; 262(1):36-55

Gradisar H, Keber MM, Pristovsek P, Jerala R. MD-2 as the target of curcumin in the inhibition of response to LPS. *J Leukoc Biol.* **2007** Oct; 82(4):968-74

Han JM, Levings MK. Immune regulation in obesity-associated adipose inflammation. *J Immunol.* **2013** Jul; 191(2):527-32

Heasman SJ, Giles KM, Rossi AG, Allen JE, Haslett C, Dransfield I. Interferon γ suppresses glucocorticoid augmentation of macrophage clearance of apoptotic cells. *Eur J Immunol.* **2004**. 34: 1752–61

Hristov M, Weber C. Differential role of monocyte subsets in atherosclerosis. *Thromb Haemost*. **2011** Nov; 106(5):757-62

Hutchinson JA, Riquelme P, Sawitzki B, Tomiuk S, Miqueu P, Zuhayra M, Oberg HH, Pascher A, Lützen U, Janssen U, Broichhausen C, Renders L, Thaiss F, Scheuermann E, Henze E, Volk HD, Chatenoud L, Lechler RI, Wood KJ, Kabelitz D, Schlitt HJ, Geissler EK, Fändrich F. Cutting edge: immunological consequences and trafficking of human regulatory macrophages administered to renal transplant recipients. *J Immunol.* **2011** Sep; 187(5):2072-8

Jaatinen T, Laine J. Isolation of mononuclear cells from human cord blood by Ficoll-Paque density gradient. *Curr Protoc Stem Cell Biol*. **2007** Jun; Chapter 2:Unit 2A.1

Jaguin M, Houlbert N, Fardel O, Lecureur V. Polarization profiles of human M-CSF-generated macrophages and comparison of M1-markers in classically activated macrophages from GM-CSF and M-CSF origin. *Cell Immunol.* **2013** Jan; 281(1):51-61

Jobin C, Bradham CA, Russo MP, Juma B, Narula AS, Brenner DA, Sartor RB. Curcumin blocks cytokine-mediated NF-kappa B activation and proinflammatory gene expression by inhibiting inhibitory factor I-kappa B kinase activity. *J Immunol.* **1999** Sep; 163(6):3474-83

Joe B, Vijaykumar M, Lokesh BR. Biological properties of curcumin – cellular and molecular mechanisms of action. *Crit Rev Food Sci Nutr*. **2004**; 44(2):97-111

Kammoun HL, Kraakman MJ, Febbraio MA. Adipose tissue inflammation in glucose metabolism. *Rev Endocr Metab Disord*. **2014** Mar; 15(1):31-44

Kawamoto T, Ii M, Kitazaki T, Iizawa Y, Kimura H. TAK-242 selectively suppresses Toll-like receptor 4-signaling mediated by the intracellular domain. *Eur J Pharmacol.* **2008** Apr; 584(1):40-8

Kraakman MJ, Murphy AJ, Jandeleit-Dahm K, Kammoun HL. Macrophage polarization in obesity and type 2 diabetes: weighing down our understanding of macrophage function? *Front Immunol.* **2014** Sep; 5:470

Lao CD, Ruffin MT 4th, Normolle D, Heath DD, Murray SI, Bailey JM, Boggs ME,Crowell J, Rock CL, Brenner DE. Dose escalation of a curcuminoid formulation. BMC Complement Altern Med. **2006** Mar;6:10

Leitinger N, Schulman IG. Phenotypic polarization of macrophages in atherosclerosis. *Arterioscler Thromb Vasc Biol.* **2013** Jun; 33(6):1120-6

Li M, Matsunaga N, Hazeki K, Nakamura K, Takashima K, Seya T, Hazeki O, Kitazaki T, Iizawa Y. A novel cyclohexene derivative, ethyl(6R)-6-[N-(2-chloro-4-fluorophenyl)sulfamoyl] cyclohex-1-ene-1-carboxylate(TAK-242), selectively inhibits toll-like receptor 4-mediated cytokine production through suppression of intracellular signaling. *Mol Pharmacol*. **2006** Apr; 69(4):1288-95

Lien E, Golenbock DT. Adjuvants and their signaling pathways: beyond TLRs. Nat *Immunol.* **2003** Dec; 4(12):1162-4

Liu L, Shang Y, Li M, Han X, Wang J, Wang J. Curcumin ameliorates asthmatic airway inflammation by activating nuclear factor-E2-related factor 2/haemoxygenase (HO)-1 signaling pathway. *Clin Exp Pharmacol Physiol*. **2015** May; 42(5):520-9

Lowry OH, Rosebrough NJ, Farr AL, Randall RJ. Protein measurement with the Folin phenol reagen; *J Biol Chem*. **1951**; 193: 265-75

Lubbad A, Oriowo MA, Khan I. Curcumin attenuates inflammation through inhibition of TLR-4 receptor in experimental colitis. *Mol Cell Biochem*. **2009** Feb; 322(1-2):127-35

Lumeng CN, Bodzin JL, Saltiel AR. Obesity induces a phenotypic switch in adipose tissue macrophage polarization. *J Clin Invest*. **2007**; 117(1):175-84

Maheshwari RK, Singh AK, Gaddipati J, Srimal RC. Multiple biological activities of curcumin: a short review. *Life Sci.* **2006** Mar; 78(18):2081-7

Mantovani A, Sica A, Sozzani S, Allavena P, Vecchi A, Locati M. The chemokine system in diverse forms of macrophage activation and polarization. *Trends Immunol* **2004** Dec; 25(12):677-86

Mantovani A, Garlanda C, Locati M. Macrophage diversity and polarization in atherosclerosis: a question of balance. *Arterioscler Thromb Vasc Biol*. **2009**; 29(10):1419-23

Mantovani A, Biswas SK, Galdiero MR, Sica A, Locati M. Macrophage plasticity and polarization in tissue repair and remodelling. *J Pathol*. **2013** Jan; 229(2):176-85

Margaritis M, Channon KM, Antoniades C. Statins as regulators of redox state in the vascular endothelium: beyond lipid lowering. *Antioxidant & Redox Signaling*, **2014**; 20(8), 1198-215

Martinez FO, Sica A, Mantovani A, Locati M. Macrophage activation and polarization. *Front. Biosci.* **2008**; 13:453-61

Martinez FO, Helming L, Milde R, Varin A, Melgert BN, Draijer C, Thomas B, Fabbri M, Crawshaw A, Ho LP, Ten Hacken NH, Cobos Jiménez V, Kootstra NA, Hamann J, Greaves DR, Locati M, Mantovani A, Gordon S. Genetic programs expressed in resting and IL-4 alternatively activated mouse and human macrophages: similarities and differences. *Blood* **2013** Feb; 121(9):e57-69

Menon VP, Sudheer AR. Antioxidant and anti-inflammatory properties of curcumin. *Adv Exp Med Biol.* 2007; 595:105-25

Mercalli A, Calavita I, Dugnani E, Citro A, Cantarelli E, Nano R, Melzi R, Maffi P, Secchi A, Sordi V, Piemonti L. Rapamycin unbalances the polarization of human macrophages to M1. *Immunology* **2013** Oct; 140(2):179-90

Mercanti G, Ragazzi E, Toffano G, Giusti P, Zusso M. Phosphatidylserine and curcumin act synergistically to down-regulate release of interleukin-1β from lipopolysaccharide-stimulated cortical primary microglial cells. *CNS & Neurological Disorders Drug Targets.* **2014**; 13(5), 792-800

Milobedzka J, Kostanecki S, Lampe V. Zur Kenntnis des Curcumins. *Deut. Chem. Ges*. **1910**; 43, 2163e2170

Moore KJ, Sheedy FJ, Fisher EA. Macrophages in atherosclerosis: a dynamic balance. *Nat Rev Immunol*. **2013** Oct; 13(10):709-21

Mosser DM, Edwards JP. Exploring the full spectrum of macrophage activation. *Nat Rev Immunol.* **2008** Dec; 8(12):958-69

Motwani MP, Gilroy DW. Macrophage development and polarization in chronic inflammation. *Semin Immunol*. **2015** Aug; 27(4):257-66

Muris AH, Damoiseaux J, Smolders J, Cohen Tervaert JW, Hupperts R, Thewissen M. Intracellular IL-10 detection in T cells by flow cytometry: the use of protein transport inhibitors revisited. *J Immunol Methods* **2012** Jul 31;381(1-2):59-65

Murray PJ, Wynn TA. Protective and pathogenic functions of macrophage subsets. *Nat. Rev. Immunol*. **2011**; 11(11):723-37

Murray PJ, Allen JE, Biswas SK, Fisher EA, Gilroy DW, Goerdt S, Gordon S, Hamilton JA, Ivashkiv LB, Lawrence T, Locati M, Mantovani A, Martinez FO, Mege JL, Mosser DM, Natoli G, Saeij JP, Schultze JL, Shirey KA, Sica A, Suttles J, Udalova I, van Ginderachter JA, Vogel SN, Wynn TA. Macrophage activation and polarization: nomenclature and experimental guidelines. *Immunity.* **2014** Jul; 41(1):14-20

Nagpal M, Sood S. Role of curcumin in systemic and oral health: an overview. *J Nat Sci Biol Med*. **2013** Jan; 4(1):3-7

Okabe Y, Medzhitov R. Tissue biology perspective on macrophages. *Nat Immunol*. **2015** Dec; 17(1):9-17

Oliveira AS, Sousa E, Vasconcelos MH, Pinto M. Curcumin: a natural lead for potential new drug candidates. *Curr Med Chem*. **2015**; 22(36):4196-232

Pabon HJJ. A synthesis of curcumin and related compounds. *Rec Trav Chim Pays Bas*. **1964**; 83, 379-86

Pello OM, Silvestre C, De Pizzol M, Andrés V. A glimpse on the phenomenon of macrophage polarization during atherosclerosis. *Immunobiology* **2011** Nov; 216(11):1172-6

Pollard JW. Trophic macrophages in development and disease. *Nat Rev Immunol***. 2009** Apr; 9(4):259-70

Priyadarsini KI, Maity DK, Naik GH, Kumar MS, Unnikrishnan MK, Satav JG, Mohan H. Role of phenolic O-H and methylene hydrogen on the free radical reactions and antioxidant activity of curcumin. *Free Radic Biol Med.* **2003** Sep; 35(5):475-84

Priyanka A, Anusree SS, Nisha VM, Raghu KG. Curcumin improves hypoxia induced dysfunctions in 3T3-L1 adipocytes by protecting mitochondria and down regulating inflammation. *Biofactors*. **2014** Sep-Oct; 40(5):513-23

Qin Z. The use of THP-1 cells as a model for mimicking the function and regulation of monocytes and macrophages in the vasculature. *Atherosclerosis*. **2012** Mar; 221(1):2-11

Repnik U, Knezevic M, Jeras M. Simple and cost-effective isolation of monocytes from buffy coats. *J Immunol Methods*. **2003** Jul; 278(1-2):283-92

Reuter S, Gupta SC, Park B, Goel A, Aggarwal BB. Epigenetic changes induced by curcumin and other natural compounds. *Genes Nutr*. **2011** May; 6(2):93-108

Schaper NC, Havekes B. Diabetes: impaired damage control. *Diabetologia* 2012; 55:18–20

Schulz C, Gomez Perdiguero E, Chorro L, Szabo-Rogers H, Cagnard N, Kierdorf K, Prinz M, Wu B, Jacobsen SE, Pollard JW, Frampton J, Liu KJ, Geissmann F. A lineage of myeloid cells independent of Myb and hematopoietic stem cells. *Science* **2012** Apr; 336(6077):86-90

Shehzad A, Rehman G, Lee YS. Curcumin in inflammatory diseases. *Biofactors*. **2013** Jan-Feb; 39(1):69-77

Sheng J, Ruedl C, Karjalainen K. Most tissue-resident macrophages except microglia are derived from fetal hematopoietic stem cells. *Immunity* **2015** Aug; 43(2):382-93

Sica A, Mantovani A. Macrophage plasticity and polarization: *in vivo* veritas. *J Clin Invest*. **2012**; 122:787-95

Singh S, Aggarwal BB. Activation of transcription factor NF-kappa B is suppressed by curcumin (diferuloylmethane) [corrected]. J Biol Chem. **1995** Oct; 270(42):24995-5000

Srivastava RM, Singh S, Dubey SK, Misra K, Khar A. Immunomodulatory and therapeutic activity of curcumin. *Int Immunopharmacol*. **2011** Mar; 11(3):331-41

Stienstra R, Duval C, Keshtkar S, van der Laak J, Kersten S, Müller M. Peroxisome proliferator- activated receptor γ activation promotes infiltration of alternatively activated macrophages into adipose tissue. *J Biol Chem*. **2008** Aug; 283(33):22620-7

Stöger JL, Gijbels MJ, van der Velden S, Manca M, van der Loos CM, Biessen EA, Daemen MJ, Lutgens E, de Winther MP. Distribution of macrophage polarization markers in human atherosclerosis. *Atherosclerosis* **2012** Dec; 225(2):461-8

Tang Z, Niven-Fairchild T, Tadesse S, Norwitz ER, Buhimschi CS, Buhimschi IA, Guller S. Glucocorticoids enhance CD163 expression in placental Hofbauer cells. *Endocrinology* **2013** Jan; 154(1):471-82

Tarique AA, Logan J, Thomas E, Holt PG, Sly PD, Fantino E. Phenotypic, functional, and plasticity features of classical and alternatively activated human macrophages. *Am J Respir Cell Mol Biol.* **2015** Nov; 53(5):676-88

Tedesco S, Bolego C, Toniolo A, Nassi A, Fadini GP, Locati M, Cignarella A. Phenotypic activation and pharmacological outcomes of spontaneously differentiated human monocyte-derived macrophages. *Immunobiology* **2015** May; 220(5):545-54

Tjiu JW, Chen JS, Shun CT, Lin SJ, Liao YH, Chu CY, Tsai TF, Chiu HC, Dai YS, Inoue H, Yang PC, Kuo ML, Jee SH. Tumor-associated macrophage-induced invasion and angiogenesis of human basal cell carcinoma cells by cyclooxygenase-2 induction. *J Invest Dermatol*. **2009** Apr; 129(4):1016-25

Tocharus J, Jamsuwan S, Tocharus C, Changtam C, Suksamrarn A. Curcuminoid analogs inhibit nitric oxide production from LPS-activated microglial cells. *J Nat Med*. **2012** Apr; 66(2):400-5

Toniolo A, Fadini GP, Tedesco S, Cappellari R, Vegeto E, Maggi A, Avogaro A, Bolego C, Cignarella A. Alternative activation of human macrophages is rescued by estrogen treatment in vitro and impaired by menopausal status. *J Clin Endocrinol Metab*. **2015** Jan; 100(1):E50-8

Vallelian F, Schaer CA, Kaempfer T, Gehrig P, Duerst E, Schoedon G, Schaer DJ. Glucocorticoid treatment skews human monocyte differentiation into a hemoglobin-clearance phenotype with enhanced heme-iron recycling and antioxidant capacity. *Blood* **2010** Dec; 116(24):5347-56

van der Meij E, Koning GG, Vriens PW, Peeters MF, Meijer CA, Kortekaas KE, Dalman RL.A clinical evaluation of statin pleiotropy: statins selectively and dose-dependently reduce vascular inflammation. *PLoS One* **2013**; 8: e53882.

van Furth R, Cohn ZA, Hirsch JG, Humphrey JH, Spector WG, Langevoort HL. The mononuclear phagocyte system: a new classification of macrophages, monocytes, and their precursor cells. *Bull World Health Organ*. **1972**; 46:845–52

Vogel H, Pelletier J. Curcumin-biological and medicinal properties. *J Pharma* **1815**; 2, 50

Vogel DY, Glim JE, Stavenuiter AW, Breur M, Heijnen P, Amor S, DijkstraCD, Beelen RH. Human macrophage polarization in vitro: maturation and activation methods compared. *Immunobiology*. **2014** Sep;219(9):695-703

Vulcano M, Albanesi C, Stoppacciaro A, Bagnati R, D'Amico G, Struyf S, Transidico P, Bonecchi R, Del Prete A, Allavena P, Ruco LP, Chiabrando C, Girolomoni G, Mantovani A, Sozzani S. Dendritic cells as a major source of macrophage-derived chemokine/CCL22 in vitro and in vivo. *Eur J Immunol*. **2001** Mar; 31(3):812-22

Wang Y, Shan X, Dai Y, Jiang L, Chen G, Zhang Y, Wang Z, Dong L, Wu J, Guo G, Liang G. Curcumin analog L48H37 prevents lipopolysaccharide-induced TLR4 signaling pathway activation and sepsis via targeting MD2. *J Pharmacol Exp Ther. 2015* Jun; 353(3):539-50

Wynn TA, Chawla A, Pollard JW. Macrophage biology in development, homeostasis and disease. *Nature* **2013**; 496, 445–55

Xue J, Schmidt SV, Sander J, Draffehn A, Krebs W, Quester I, De Nardo D, Gohel TD, Emde M, Schmidleithner L, Ganesan H, Nino-Castro A, Mallmann MR, Labzin L, Theis H, Kraut M, Beyer M, Latz E, Freeman TC, Ulas T, Schultze JL. Transcriptome-based network analysis reveals a spectrum model of human macrophage activation. *Immunity.* **2014** Feb; 40(2):274-88

Yang M, Zheng J, Miao Y, Wang Y, Cui W, Guo J, Qiu S, Han Y, Jia L, Li H, Cheng J, Du J. Serum- glucocorticoid regulated kinase 1 regulates alternatively activated macrophage polarization contributing to angiotensin II-induced inflammation and cardiac fibrosis. *Arterioscler Thromb Vasc Biol*. **2012** Jul; 32(7):1675-86

Youn HS, Saitoh SI, Miyake K, Hwang DH. Inhibition of homodimerization of Toll-like receptor 4 by curcumin. *Biochem Pharmacol*. **2006** Jun; 72(1):62-9

Zhou Y, Zhang T, Wang X, Wei X, Chen Y, Guo L, Zhang J, Wang C. Curcumin modulates macrophage polarization through the inhibition of the toll-like receptor 4 expression and its signaling pathways. *Cell Physiol Biochem*. **2015**; 36(2):631-41

Ziegler-Heitbrock L, Ancuta P, Crowe S, Dalod M, Grau V, Hart DN, Leenen PJ, Liu YJ, Mac Pherson G, Randolph GJ, Scherberich J, Schmitz J, Shortman K, Sozzani S, Strobl H, Zembala M, Austyn JM, Lutz MB. Nomenclature of monocytes and dendritic cells in blood. *Blood.* **2010** Oct; 116(16):e74-80